

**MESOSCALE FORCING, PHYTOPLANKTON
COMMUNITY STRUCTURE AND SIZE CLASS
DISTRIBUTION IN THE CARIBBEAN**

by

Helena Antoun Kučerova

A thesis submitted in fulfillment of the requirements for the degree of

MASTER OF SCIENCE
in
Marine Sciences

UNIVERSITY OF PUERTO RICO
MAYAGÜEZ CAMPUS
2009

Approved by:

Jorge E. Corredor, PhD
Member, Graduate Committee

Date

Julio M. Morell, PhD
Member, Graduate Committee

Date

José M. López, PhD
Member, Graduate Committee

Date

Wei Wei, PhD
Representative of Graduate Studies

Date

Nilda Aponte, PhD
Director of the Department

Date

COPYRIGHT

In presenting this dissertation in partial fulfillment of the requirements for a Master in Marine Sciences degree at the University of Puerto Rico, I agree that the library shall make its copies freely available for inspection. I therefore authorize the Library of the University of Puerto Rico at Mayaguez to copy my MS Thesis totally or partially. Each copy must include the title page. I further agree that extensive copying of this dissertation is allowable only for scholarly purposes. It is understood, however, that any copying or publication of this dissertation for commercial purposes, or for financial gain, shall not be allowed without my written permission.

Signed: Helena Antoun

Date: 4/13/09

Abstract

Mesoscale phenomena influence phytoplankton community composition, size class distribution, abundance and photosynthetic capacity, in turn determining food web structure. As this structure influences carbon sequestration in the oceans, mesoscale forcing affects carbon sequestration capacity. This study was conducted to characterize phytoplankton community structure and size class distribution based on HPLC-assisted chemotaxonomy of size fractionated samples from different environments in the eastern Caribbean under the influence of the Orinoco River plume and mesoscale eddies.

Little response to the effect of cyclonic and anticyclonic eddies in phytoplankton population and abundance was observed. However, a slight increase in pico and nanoplankton biomass was noted, with values higher in the cyclonic region than the anticyclonic region. Oligotrophic oceanic waters were found to be mostly dominated by pico and nanoplankton populations. However, increased river plume influence resulted in reduced proportional biomass of both nano and picoplankton and corresponding increase in microplankton.

Chemotaxonomic analyses of size fractionated samples show significant overlap of diagnostic pigments across the micro, nano and pico size spectrum indicating that size structure cannot be inferred solely by photosynthetic pigment identification. If specific size structure of phytoplanktonic populations is in question, sequential filtration using designated pore sizes coupled with HPLC is suggested.

Resumen

Los fenómenos de meso escala influyen la composición poblacional del fitoplancton, su distribución de clases por tamaño, su abundancia y su capacidad fotosintética, lo cual determina la estructura de la red alimentaria. Como estas estructuras influyen la captura de carbono en los océanos, la capacidad de la captura es afectada por los fenómenos de meso escala. Este estudio fue diseñado para caracterizar las comunidades de fitoplancton y su distribución de tamaño usando el método de quimotaxonomía a través de HPLC para muestras fraccionadas por tamaño de distintos ambientes del este del Caribe bajo la influencia de la descarga del Río Orinoco y los remolinos de meso escala.

Se observó poco cambio en abundancia y composición de poblaciones fitoplanctónicas con respecto a los efectos de los remolinos ciclónicos y anticiclónicos, aunque se notó un leve aumento en biomasa de pico y nanoplancton en las regiones ciclónicas. Las aguas oligotróficas del mar Caribe fueron dominadas por poblaciones de pico y nanoplancton. Sin embargo, la influencia de la descarga del río resultó en una disminución de contribución proporcional de poblaciones de pico y nanoplancton coincidente con aumentos en la contribución proporcional del microplancton.

Análisis quimotaxonomías de muestras que fueron fraccionadas por tamaño demuestra un solapamiento significativo de pigmentos diagnósticos a través del rango de tamaños de micro, nano y pico, indicando que la estructura de los tamaños fitoplanctónicos no se puede determinar exclusivamente usando la quimotaxonomía. Si se desea determinar los tamaños específicos para las poblaciones fitoplanctónicas se recomienda filtración secuencial con filtros de poros designado junto con análisis de HPLC.

Acknowledgements

I would like to express my sincerest gratitude to my advisor, Dr. Jorge Corredor, for giving me the opportunity to work with him and his team and consequently embarking on many unforgettable ocean adventures. For all his time, patience, immediate assistance in everything, I am deeply grateful.

I would also like to thank my committee members, Dr. José López (Papo) and Professor Julio Morell for all their help, advice, encouragement and good humor throughout the years. Dr. Nilda Aponte for all her advice and support. The crew of the R/V Chapman and R/V Pelican for all their assistance, support and great company. My lab mates and friends, who have helped me in countless ways throughout the years.

I would also like to thank my Mom and Dad for all their enthusiasm, encouragement and support.

This research was supported by the Office of Science (BER), the U.S. Department of Energy, and the Office of Naval Research (grants No. DE-FG02-05ER64149, DE-FG02-05ER64029 and N000140310904 respectively).

Table of Contents

Abstract.....	iii
Resumen.....	iv
Acknowledgements.....	v
Table of Contents.....	vi
List of Tables.....	viii
List of Figures.....	ix
I. Introduction.....	1
II. Literature Review.....	5
Carbon flux.....	5
Influence of mesoscale processes on phytoplankton community composition.....	6
Methods of analysis.....	15
III. Objectives.....	18
IV. Methodology.....	19
Experimental Design.....	19
Seawater Collection.....	20
Phytoplankton Extraction.....	21
Instrumental analysis.....	22
Materials and instrumentation.....	23
Quality control.....	24
V. Results.....	26
Physical characteristics.....	26
Phytoplankton pigment distribution.....	29
Phytoplankton community structure as inferred from bulk sample pigment composition.....	33
<i>Influence of river plume.....</i>	33
<i>Influence of meso-scale eddies.....</i>	36
Phytoplankton size distribution as derives from sequential and fractionated filtration.....	36
VI. Discussion.....	40
Influence of meso-scale phenomena on phytoplankton population distribution.....	40
Size fractionation of phytoplankton populations.....	47

	Comparison pigment based estimation of phytoplankton size-class distribution to sequential filtration results.....	54
	Determining proportional recovery of fractionated samples.....	57
VII.	Conclusions.....	59
VIII.	References.....	60

List of Tables

Table 1. Pigment ratio to Chl <i>a</i> for five taxonomic pigments (Fucoxanthin, 19'-Butanoyloxyfucoxanthin, 19'-Hexanoyloxyfucoxanthin, Zeaxanthin and Chlorophyll <i>b</i>).....	11
Table 2. Standard taxonomic pigments.....	16
Table 3. Dates, coordinates, (decimal degrees), salinity values and respective abbreviations for stations sampled.....	20
Table 4. Parameter values used for the HPLC.....	23
Table 5. Mobile phase parameters used for the HPLC.....	23
Table 6. Proportional distribution of surface taxonomic pigments within the size fractions..	39
Table 7. Proportional distribution of DCM taxonomic pigments within the size fraction.....	39

List of Figures

Figure 1. K490MODIS satellite imagery of the Orinoco River Plume extending across the Caribbean Sea.....	7
Figure 2. Pattern of flow for the North Brazilian Current (NBC) and other major currents in the Caribbean Sea.....	12
Figure 3. Schematic diagram of sea surface height and isopycnal displacement induced by cyclonic and anticyclonic rotation in the ocean.....	13
Figure 4. Cruise track.....	19
Figure 5. Near-surface salinity and KdPAR values with respect to distance from the Orinoco River Plume.....	27
Figure 6. Depth of the deep chlorophyll maximum (DCM) along the distance gradient of the Orinoco River Plume (ORP).....	27
Figure 7. Spatial distribution of KdPAR and near surface Chl a concentrations along the river plume.....	28
Figure 8. Sea surface height altimetry (SSHA) for stations Cav3, Cav8, Cav11, Cav16, Cav20 and Cav23.....	28
Figure 9. Surface pigment concentrations and distribution along the salinity gradient.....	30
Figure 10. DCM pigment concentrations and distribution in relation to the surface salinity gradient.....	30
Figure 11. Pigment distribution along the KdPAR gradient.....	31
Figure 12. DCM pigment concentration for stations Cav3, Cav8 and Cav11.....	32
Figure 13. DCM pigment concentration for sations Cav16, Cav20 and Cav23.....	32
Figure 14. Distribution of taxonomic pigments along surface salinity gradient-Microplankton and nanoplankton.....	34
Figure 15. Distribution of taxonomic pigments along surface salinity gradient-Nanoplankton and picoplankton.....	35
Figure 16. Distribution of taxonomic pigments along surface salinity gradient-Microplankton and picoplankton.....	35

Figure 17. Distribution of surface taxonomic pigment concentration within the size fraction along the surface salinity gradient.....	37
Figure 18. Distribution of DCM taxonomic pigment concentration within the size fraction along the surface salinity gradient.....	38
Figure 19. Chemotaxonomic pigment ratios calculated with respect to Chl <i>a</i> within the deep chlorophyll maxima (DCM).....	42
Figure 20. Surface pigment ratios (pigment/Chl <i>a</i>) along the surface salinity gradient.....	45
Figure 21. DCM pigment ratios along the surface salinity gradient.....	46
Figure 22. Surface biomass proportion.....	47
Figure 23. Ratios of surface sample taxonomic marker pigments to Chl <i>a</i> within the size fraction.....	51
Figure 24. Ratios of taxonomic marker pigments to Chl <i>a</i> within the size fraction.....	52
Figure 25. Proportion of taxonomic marker pigments within the operational size ranges contrasted to pigment-based size classification.....	53
Figure 26. Estimated and fractionated microplankton Chl <i>a</i> biomass proportions – Microplankton.....	55
Figure 27. Estimated and fractionated microplankton Chl <i>a</i> biomass proportions – Nanoplankton.....	56
Figure 28. Estimated and fractionated microplankton Chl <i>a</i> biomass proportions – Picoplankton.....	56
Figure 29. Proportional recovery values for Chl <i>a</i>	58

I. Introduction

Phytoplankton makes up about 25% of the planet's vegetation. It is the building block of all animal production in the open sea supporting the food webs in which the world's fisheries are based on (Jeffery et al., 1997) and plays an important role in the partitioning of carbon within the food web structure which governs the magnitude and efficiency of carbon cycling in the ocean and the flow of energy to higher trophic levels in the food chain (Rivkin et al., 2002). Phytoplankton is commonly divided into three ecologically relevant size classes: microplankton ($>20 \mu\text{m}$), nanoplankton ($20\text{-}2 \mu\text{m}$) and picoplankton ($2\text{-}0.2 \mu\text{m}$) (Sieburth et al., 1978). The microplankton fraction is usually made up of diatoms and dinoflagellates. The nanoplankton fraction of chromophytes and cryptophytes, while the picoplankton fraction is usually made up of cyanobacteria, green flagellates and prochlorophytes (Sieburth et al., 1978; Gieskes et al., 1988; Vidussi et al., 2001).

Carbon sequestration in the deep ocean plays a key role in the partitioning of carbon in the form of carbon dioxide between the ocean and atmosphere, influencing past and present climate changes (EDOCC, 2001). Biological sequestration, better known as the biological pump, is the result of a complex biologically interacting network (eg. grazing of zooplankton on phytoplankton) responsible for the export of carbon through photosynthetic fixation and subsequent sinking of organic particles. These processes remove carbon from surface waters and transport it to the deep ocean where it can be remineralized and isolated from the atmosphere (McGuillicuddy et al., 2007) and are mediated principally by the larger size classes which zooplankton can effectively transform into rapidly sinking particles. Picoplankton have been known to fuel the microbial food web (MFW) which is perceived to "short circuit" the particulate carbon (C) pump by converting most of this C into CO_2 (Rivkin

et al., 2002). As an example, in a conceptual food web model described by Legendre and Rivkin (2002) phytoplankton, the MFW and zooplankton were described as the three parameters that controlled the cycling of biogenic carbon in the upper ocean. Particularly, the bacterial component of the MFW was found to be responsible for essentially all the remineralization of biogenic carbon, mainly of phytoplankton origin, to CO₂. It is estimated that every year oceanic phytoplankton generate 40 x 10¹⁵ g of fixed carbon, while coastal macroalgae generate an extra 4 x 10¹⁵ g of fixed carbon per year. This is currently about 50-100% of the primary productivity of terrestrial ecosystems (Graham et al., 2000).

Microplanktonic diatoms play an important role in carbon flux as they are large and thus can be grazed upon by large zooplankters which in turn produce large, rapidly sinking fecal pellets. Tropical diatoms *Rhizosolenia* and *Hemiaulus* play a further important role due to their symbiotic relationship with the nitrogen fixing cyanobacterium *Richelia* (Foster et al., 2007). Nitrogen fixed by these symbiotic pairs can fuel further production and carbon sequestration when nitrogen is limiting under which circumstances diatoms usually play a minor role. Diatoms and coccolithophores, the latter members of the picoplankton, are known as “ballasted species”; organisms with mineral inclusions which further contribute to rapid sedimentation. These also play an important role in the sequestration of organic carbon via natural aggregation and the production of “marine snow”. Picoplanktonic cyanobacteria are nitrogen fixers and were the first organisms to sequester inorganic carbon from the atmosphere and oxygenate the atmosphere via photosynthesis 2.7 billion years ago (Graham et al., 2000).

Phytoplankton community composition is dependent on temperature, light and the availability of macro and micro nutrients. These are important parameters that affect growth

and dynamics (Rivkin et al., 2002). Climate processes and mesoscale phenomena such as river discharge, upwelling and island mass effect are factors that influence the above parameters (Bidigare et al., 1993; Corredor et al., 2003; Steinberg et al., 2001; Vaillancourt et al., 2003; Sander et al., 1981; Corredor et al., 1984). Traditional methods for the study of community composition and size structure of phytoplankton populations were largely limited to light microscopy. These methods however proved to be time consuming in terms of sample treatment, identification and training (Li et al., 2002) and, until the development of epi-fluorescence microscopy, largely overlooked the picoplankton component. Instead chemotaxonomy, the identification of phytoplankton community composition based on characteristic (or taxonomic) photosynthetic and photoprotective pigments, became popular (Anderson et al., 1996; Vidussi et al., 2001; Li et al., 2002). Not only did this method provide a quicker way of characterizing phytoplankton community composition, but since it is generally understood that certain classes fall under specific size ranges, by identifying taxonomic pigments it was also possible to map the size structure of the population (Bidigare et al., 1993; Jeffery et al., 1997; Vidussi et al., 2001; Li et al., 2002). Hence, chemotaxonomic identification using high performance liquid chromatography (HPLC) became a standard method for identifying community composition and size class distribution (Jeffery et al., 1997).

Caribbean waters are under the strong influence of river plumes, island mass effect and meso-scale eddies which, as noted above, have significant influence on community composition (Bidigare et al., 1993; Corredor et al., 1984; Corredor et al., 2003) but little is known or has been done to characterize phytoplankton size structure and community composition in the Caribbean and most of what has been done is an estimate on the

ecological characterization of phytoplankton communities based solely on the presence of taxonomic pigments. This method does not give an entirely accurate description of size structure since, for example, classes that fall under the micro-fraction can in fact be present in the nano-fraction (eg. diatoms). In order to better understand food web structure and global carbon flux it is important to better understand relationship between meso-scale phenomena and phytoplankton size structure along with the community composition. This study was undertaken with the goals of better understanding the influence of mesoscale phenomena on phytoplankton community composition and further clarifying the relationship between phytoplankton chemotaxonomy and size distribution in the region.

II. Literature Review.

Carbon flux

In order to understand the role phytoplankton play in the oceans, it is important to understand the parameters that influence phytoplankton growth and production and the size class distribution of phytoplankton in the oceans since these parameters determine the different carbon pathways. Decomposing algae, a source of organic carbon, is converted by aquatic bacteria into decay resistant colloids which is made up of dissolved and particulate organic carbon. About 20% of the total dissolved organic carbon (DOC), which equates to approximately 30% of the total global annual primary productivity, in surface waters occurs as acylpolysacchrides (APS). APS aggregate with bacteria, zooplankton remains and fecal pellets to form marine snow. Phytoplankton are the only known source of APS, producing a global reserve of 10-15 gigatons- diatoms being a well documented producer of APS (Graham et al., 2000).

The most abundant filamentous specie, *Trichodesmium sp.*, mass together to form free floating colonies and are known to thrive in low nutrient oligotrophic waters. Picoplankton account for a large portion of primary production (70% or more) in oligotrophic waters (Richardson et al., 2007). They can be responsible for an 89-90% annual carbon production. Picoplankton is grazed upon by flagellates, ciliates, rotifers, copepods and metazoans and hence contributing to the flow of energy to higher trophic levels (Stockner, J.G., 1988).

In 1979 Richard Eppley and Bruce Peterson developed a method for estimating carbon sequestration using the f-ratio (Ducklow et al., 2001), which is calculated by dividing the amount of new primary production (primary production fueled by nitrate) with that of

total primary production (primary production fueled by other sources of nitrogen such as ammonia). The f-ratio estimates the flux of sinking particulate organic carbon as a direct function of nitrate flux to surface waters with that, so as to give an idea of how much carbon is being sequestered in the ocean and isolated from the atmosphere. To fully understand the role these biological processes have on influencing our atmospheric carbon concentrations and therefore our climate, we need to understand the basic mechanisms of the biological pump. One way of doing that is by understanding phytoplankton size and community structure.

Influence of mesoscale processes on phytoplankton community composition

Seasonal variations in biomass and primary productivity are observed in the eastern Caribbean basin in response to variations in nutrient concentration, salinity and phytoplankton class distribution and concentration due to river discharge carrying nutrients and organic material (dissolved and particulate), and mesoscale eddies (Morell et al., 2001; Bricaud et al., 2004; Guzman-Bustillos et al., 1995; Bidigare et al., 1993; Barlow et al., 1993).

The Amazon, Magdalena and Orinoco Rivers are responsible for approximately 20% of the world's annual riverine input into the oceans (Bidigare et al., 1993). Variability in rainfall over the Orinoco River Plume (ORP) has been found to significantly influence phytoplankton pigment composition, *Chl a* concentrations and depth of the deep chlorophyll max (DCM) in the Caribbean. Satellite imagery shows that the Orinoco river plume extends seasonally across the Caribbean basin (Fig. 1). Ocean color imagery also shows the Orinoco River plume mostly confined within the Antilles island arc while the Amazon River plume

spreads north outside the arc and eventually flows into the eastern Caribbean and north along the outer edge of the great Antilles. Hence, it is the Orinoco River that accounts for most of the late fall fresh water input, and nutrient loading in the Caribbean. As a result, the Orinoco river plume is responsible for the maintenance of the high near surface phytoplankton biomass within the Caribbean Atlantic front (Corredor et al., 2003).

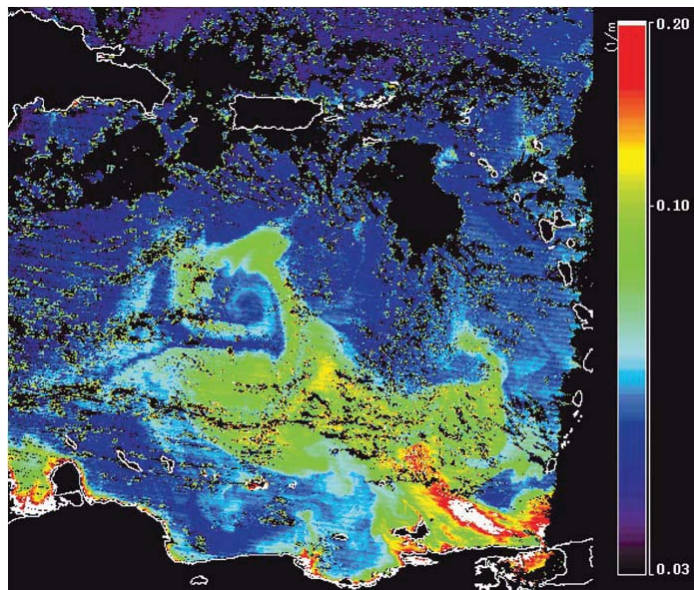


Figure 1. K490MODIS satellite imagery of the Orinoco River Plume extending across the Caribbean Sea. In this image a cyclonic eddy can be seen interacting with the plume as it propagates westward along the Caribbean. (Corredor et al., 2004)

Studies from 1994 to 2005 at the Caribbean Time Series station (CaTS) off the south coast of Puerto Rico have found seasonal variations in chemical features of the upper water masses of the North Eastern Caribbean (Corredor et al., 2001). Among the seasonal variabilities were periodic surface salinity depressions in the fall of each year coupled with increased dissolved silicate content. Studies at CaTS have also shown that phytoplankton stocks and their vertical distribution in eastern Caribbean Surface waters vary throughout the

year. These variations coincided with the fresh water input coming from the Amazon and Orinoco Rivers whose fresh water plumes are transported across the Caribbean, a transport commonly modulated by mesoscale eddies (Corredor et al., 2004).

In the Gulf of Paria where the Orinoco River outreaches the ocean, Morell and Corredor (2001) reported *Chla* values that reached up to $3.2 \text{ mg}\cdot\text{m}^{-3}$ and farther away from the river's mouth in the southeastern Caribbean near latitude 11 *Chla* concentrations dropped to $1.7 \text{ mg}\cdot\text{m}^{-3}$. Yet, this concentration in *Chla* was still higher than the average chlorophyll *a* values during times of minimum riverine influence ($0.089 \text{ mg}\cdot\text{m}^{-3}$).

Bidigare et al. (1993) reported a shoaling of the DCM for stations influenced by the river plume and a shift in phytoplankton population structure. For stations influenced by the river plume, the depth of the DCM was found to be $39 \pm 16 \text{ m}$ with a phytoplankton population dominated by diatoms whereas for stations not under the influence of the river, DCM was reported at $77 \pm 12 \text{ m}$ with a phytoplankton population comprised of cyanobacteria and possibly prochlorophyte-like cells. There was also significant variability in phytoplankton population composition for samples taken in near shore stations under the influence of the river during wet and dry seasons. During the dry seasons high concentrations of zeaxanthin were found followed by 19'-hexanoyloxyfucoxanthin (19'-HF), fucoxanthin (fuco) and finally 19'-butanoyloxyfucoxanthin (19'-BF). During the wet season a shift was observed in marker pigments where fucoxanthin was the dominant pigment followed by 19'-HF, zeaxanthin, and finally 19'-BF. This would imply that, due to nutrient loading from the river during wet seasons, hydrographic conditions favor the larger microplankton class whereas during seasons of low nutrient output conditions favor the picoplankton class. What is interesting to note here is that the population shifts would occur mostly between the

microplankton and picoplankton fractions. Bidigare et al. concludes that nutrient loading, elevation of absorption and attenuation coefficients, and transport of coastal phytoplankton populations are possible mechanisms by which the Orinoco River modifies the composition and distribution of phytoplankton in the Caribbean.

Corredor and Morell (2001) observed the influence of the ORP in a study conducted to document vertical and temporal variations of water mass structure, dissolved nutrients, phytoplankton Chl a , and dissolved organic matter at the Caribbean Time Series Station (CaTS) off the southern coast of Puerto Rico, with an emphasis on Caribbean Surface Waters (CSW). This study found that the influence of the ORP extended as far north as CaTS since the low salinity, high silicate content and seasonal shoaling of the DCM found within the CSW at CaTS correlated with the average rainfall over the Orinoco River Basin.

Observations have been noted in other regions where coastal upwelling and vertical transport of nutrients increase nutrient content and availability, while population structure has been found to be sensitive to hydrographic conditions such as water column stratification. Guzmán-Bustillos et al. (1995) found that in the Mediterranean picoplankton (cyanobacteria and prochlorophytes) were sensitive to water column mixing and favored well stratified waters. Nanoplankton were found to be the most abundant under a variety of conditions and seemed adaptable to various water column structures and microplankton (diatoms) bloomed under semi mixed conditions.

In an expedition spanning the Atlantic basin from the United Kingdom to the Falkland Islands (50°N to 50°S), Marañón et al. (2001) characterized the patterns of phytoplankton size structure and productivity in temperate, oligotrophic, upwelling and equatorial regions. In their study they found that picoplankton accounted for 56% of the total

integrated carbon fixation and 71% of the autotrophic biomass, while enhanced biomass and productivity by nano and microplankton fractions took place in temperate regions and in the upwelling area off Mauritania. Marañon et al. (2001) also noted that most of the latitudinal variability in total photoautotrophic biomass and production was driven by changes in the picoplankton fraction. In regions influenced by the Mauritania upwelling, picoplankton DCM *Chl a* values were reported to reach $0.4 \text{ mg} \cdot \text{m}^{-3}$ and microplankton *Chl a* values were above $0.2 \text{ mg} \cdot \text{m}^{-3}$. While in comparison, the lowest *Chl a* values in the oligotrophic gyres were reported to be less than $0.1 \text{ mg} \cdot \text{m}^{-3}$. Within the euphotic layer in tropical and subtropical waters, and in the upper mixed layer in the equatorial region the *Chl a* concentration within the nanoplankton fraction was below $0.05 \text{ mg} \cdot \text{m}^{-3}$. The highest nanoplanktonic *Chl a* values were found to be in surface and subsurface temperate waters with values ranging between $0.2\text{-}0.3 \text{ mg} \cdot \text{m}^{-3}$.

In a study performed to compare the taxonomic composition of phytoplankton in two sets of oligotrophic field samples within the Atlantic and Pacific Oceans (Anderson et al., 1996), HPLC pigment analysis was used to determine the pigment signatures and hence, phytoplankton population structure of those regions. Hydrostation S at the Bermuda Time Series Station (BaTS) ($32^{\circ}10' \text{N}$, $64^{\circ}30' \text{W}$) served as the sample site for the Atlantic Ocean oligotrophic sample. For Hydrostation S, surface and DCM phytoplankton populations appear to be dominated by the nano and picoplankton fractions. Surface (20 m) and DCM (120 m) pigment ratios with respect to *Chl a* of the five marker pigments (fucoxanthin, 19'-BF, 19'-HF, zeaxanthin and chlorophyll *b*) are given in Table 1.

Table 1. Pigment ratio to Chl *a* for five taxonomic pigments (fucoxanthin, 19'-butanoyloxyfucoxanthin, 19'-hexanoyloxyfucoxanthin, zeaxanthin and chlorophyll *b*). Data was derived from Table 3-Anderson et al., 1996.

Depth (m)	Fuco	19'-BF	19'-HF	Zeax	Chl<i>b</i>
20	0.0441	0.0735	0.294	0.217	0.036
120	0.0251	0.181	0.304	0.137	0.660

From this data it is apparent that the microplankton population contributed less than the smaller nano and picoplankton populations to the phytoplankton biomass of oligotrophic regions in the Atlantic Ocean. Anderson's results, when compared to the results of upwelling regions and regions influenced by the ORP, help to demonstrate the dynamics of phytoplankton size class distribution with the availability of nutrients.

Mesoscale eddies are large whirlpools in the oceans with diameters of hundreds of kilometers. Their influence can extend to depths of 1000m or greater. They can either rotate in a cyclonic (counterclockwise) or anticyclone (clockwise) pattern. Caribbean anticyclonic eddies originate from Atlantic eddies known as North Brazil Current Rings (NBCR), which in turn originate from instabilities in the North Brazilian Current (NBC) retroflection (Philander, G.S., 1990). Figure 2 shows the pattern of flow for the North Brazil Current and other major currents in the Caribbean.

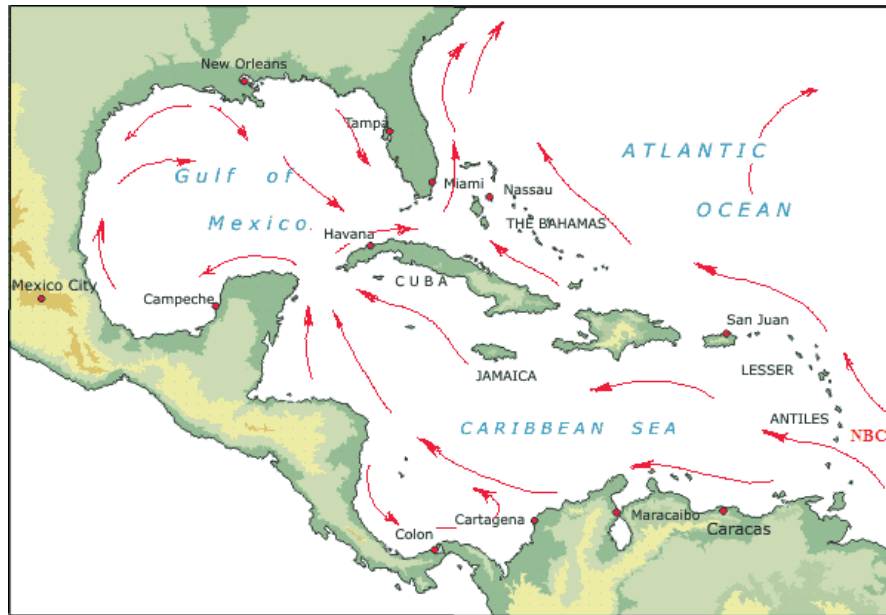


Figure 2. Pattern of flow for the North Brazilian Current (NBC) and other major currents in the Caribbean Sea. (http://www1yachtua.com/caribbean_sailing_maps/caribbean_sea_current_map.gif)

Eddies are baroclinic, transport potential and kinetic energy, nutrients and biota. In the case of cyclonic eddies, a divergent surface flow is created at their margins which induces a negative sea-surface height anomaly in the eddy center. This induces an upward displacement of deep colder water along constant density surfaces. As a result, there is an upward displacement of the nutricline, bringing new nitrogen and other nutrients into the euphotic zone (Fig. 3). Coupled with an enhancement in the vertical and horizontal flux, an upwelling of deeper nutrient rich waters are spread out around the eddy causing an increase in biogenic reactivity, primary productivity, phytoplankton photosynthetic quantum efficiency and phytoplankton growth rates (Karger-Muller et al., 1994; Smith et al, 1996; Corredor et al, 2003; Ducklow et al., 2001; Vaillancourt et al., 2003).

On the other hand, anticyclones display convergent surface flow at their margins creating a positive sea surface height anomaly at the core which induces downward

displacement of the isopycnals and hence, downward displacement of the nutricline. This downwelling is usually associated with low productivity since nutrients are pushed down into deeper waters away from the euphotic zone. However, anticyclonic eddies can be responsible for the upwelling of nutrients around the eddy core caused by perturbations in the circular flow of the eddy. Yet, the mechanisms by which eddies propagate and transfer nutrients from deeper waters into the euphotic zone is still not entirely understood.

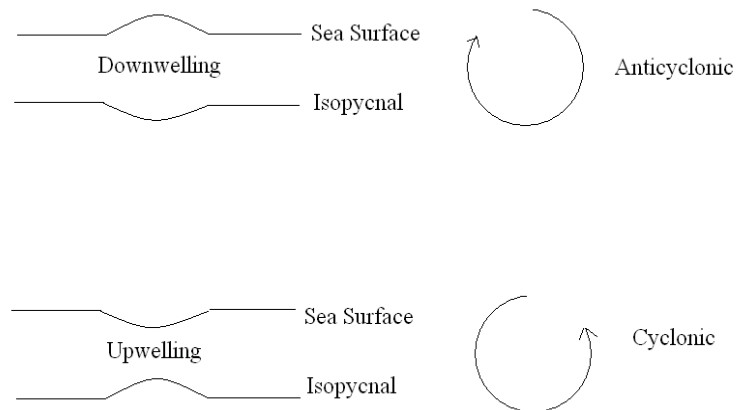


Figure 3. Schematic diagram of sea surface height and isopycnal displacement induced by cyclonic and anticyclonic rotation in the ocean.

Several studies performed in cyclonic and anticyclonic eddies and their influence on phytoplankton populations demonstrate the dynamics between nutrient availability and phytoplankton size class distribution. Analogous to the Orinoco River Plume entrainment with eddies in the Caribbean, a study done at the Prince Edward Island Plateau, Canada, showed that available nutrient concentrations are locally enhanced by run-off water retained by an eddy field which in turn induces a phytoplankton bloom within the eddy (Perissintto et

al., 1990). While in the oligotrophic Atlantic gyres there are regions where nutrients are brought to surface waters and induce a plankton bloom. McGuillicuddy et al. (1998) and Oschlies et al. (1998) proposed that such events are due to cyclonic eddies which induce an upwelling of the nutricline. Similar observations have been noted in other studies done in the Atlantic Ocean and other regions such as the Mediterranean and Pacific Ocean.

Although anticyclonic eddies are characterized by downwelling of the nutricline, there have been cases documenting the increase of biological productivity within these regions. In the Southern Bay of Biscay, France, an anticyclonic eddy was found to have a two fold increase in Chl a concentration within the eddy relative to surrounding waters. A phytoplankton population shift was also observed with the larger microplankton (diatoms) confined mostly to the eddy center and the smaller picoplanktonic population found mostly outside the eddy. In another study of an anticyclonic eddy, Martin et al. (2001, 2003) found patches of phytoplankton blooms around the eddy centre. Martin et al. proposed that these patches were due to perturbations that would cause ripples in the eddy, inducing vertical mixing and hence, an upwelling of nutrients. Causes of perturbations could be from self propagation, instability and decay, storms and topography.

Vaillancourt et al. (2003) conducted hydrographic surveys and biomass analysis on cyclonic eddies in the subtropical North Pacific. Surface waters in the eddy center was 3.5°C cooler, 0.5 saltier and 1.4 kg·m⁻³ denser than surface waters outside the eddy, indicative of upwelling. Nutrient concentrations (nitrate/nitrite, phosphate and silicate) were enhanced within the eddy by a two fold increase relative to waters outside the eddy. Chlorophyll a concentrations were higher within the eddy (greater than 33 mg·m⁻²) when compared to control stations outside the eddy (between 21-31 mg·m⁻²). Due to high nutrient availability

within the eddy center, a high accumulation of larger phytoplankton species (eukaryotes, $>3\mu\text{m}$ in diameter) were observed. In contrast, photosynthetic bacteria (*Prochlorococcus* and *Synechococcus*) and smaller photosynthetic eukaryotes ($< 3\mu\text{m}$ in diameter) were 3.6-fold more abundant outside the eddy as compared to the inside.

Vidussi et al. (2001) compared anticyclonic with cyclonic gyres in the Eastern Mediterranean and reported that the highest total *Chl a* concentrations ($\sim 40.3 \text{ mg}\cdot\text{m}^{-2}$) with the highest microplankton contribution (up to 26% of total *Chl a*) was found in the cyclonic gyres relative to the anticyclonic gyre. The anticyclonic gyres were characterized by low total *Chl a* concentrations ($\sim 19 \text{ mg}\cdot\text{m}^{-2}$) and the highest picoplankton contribution ($\sim 40\%$ of the total *Chl a*) whereas the core of the cyclonic gyre was dominated by microplankton (mainly diatoms), and adjacent areas were characterized by high *Chl a* concentrations dominated by pico and nanoplankton.

Methods of analysis

Chemotaxonomy is performed by identifying specific marker pigments using HPLC coupled with a detector that can measure the absorption spectrum of the pigments such as the diode array detector (DAD). Using HPLC coupled with a DAD the presence and concentration of taxonomic marker pigments can be detected and hence, the biomass fraction of specific phytoplankton classes can be calculated (Moore et al., 1995; Vidussi et al., 2001; Uitz et al., 2006). Table 2 gives the different marker pigments associated with each phytoplankton class. However, it must be noted that in some cases traces of marker pigments can be found in more than one class (Anderson et al., 1996; Vidussi et al., 2001; Uitz et al., 2006).

Table 2. Standard taxonomic pigments (Vidussi et al., 2001)

Pigments	Abbreviation	Taxonomic Significance	Size (μm)
Zeaxanthin	Zeax	Cyanobacteria and Prochlorophytes	< 2
Chlorophyll <i>b</i>	Chl <i>b</i>	Green Flagellates and Prochlorophytes	< 2
19'-Hexanoyloxyfucoxanthin	19'-HF	Chromophytes nanoflagellates	2- 20
19'-Butanoyloxyfucoxanthin	19'-BF	Chromophytes nanoflagellates	2- 20
Alloxanthin	Allox	Cryptophytes	2- 20
Fucoxanthin	Fuco	Diatoms	> 20
Peridinin	Peri	Dinoflagellates	>20

The analysis of phytoplankton population and size class structure via HPLC is usually done by following the standard method of analysis developed by Jeffery et al. (1997) or a similar variation where the water samples are filtered using Whatman glass fiber GF/F filters which have a pore size of approximately $0.7\mu\text{m}$ (Vidussi et al., 2001.; Anderson et al., 1996.; Bidigare et al., 1993). There are a few drawbacks to this method. First, many of the smaller celled picoplankton are lost through the pores of the GF/F filters. Second, as stated earlier, the pigment derived classes defined do not strictly refer to the true size of the phytoplankton. Alternatively, these inaccuracies can be addressed by coupling HPLC analysis with microscopic analysis (classical and/or scanning electron microscopy), or filtering water samples by tandem or sequential fraction filtration. It is worth mentioning that new methods are being developed to characterize phytoplankton populations based on RNA characterization (Wawrik and Paul, 2004) and absorption properties (Marra et al., 2007; Bricaud et al., 2004). Since a population may be defined by its pigment composition, and this

in turn is determinant of phytoplankton absorption properties, the response of phytoplankton community structure to environmental factors can be measured from absorption variations. Marra et al. (2007) and Bricaud et al. (2004) both proposed mathematical models to calculate phytoplankton absorption and hence, estimate the size structure of algal populations. The advantage of such models is in the ability to characterize phytoplankton populations from satellite-based reflectance imagery.

III. Objectives

Other than the work of Bidigare et al. (1993) and Cárdenas (2006, unpublished), little is known regarding pigment content or size class composition of Caribbean phytoplankton communities. In the Caribbean, seasonal variations occur throughout the years in terms of nutrient concentration and salinity under the influence of various meso-scale phenomena including river plumes and eddy upwelling. These variations influence phytoplankton taxonomy, size class distribution, abundance and photosynthetic capacity in turn determining plankton community composition and food web structure. Moreover, as phytoplankton community composition influences organic carbon transport and sequestration in the oceans, such mesoscale forcing is expected to affect carbon sequestration capacity in the region.

The purpose of this investigation was to corroborate the results of Bidigare et al. (1993), to further characterize phytoplankton composition and distribution in different environments of the eastern Caribbean and to assess photosynthetic pigment distribution in ecologically relevant size fractions in waters of the eastern Caribbean basin under the influence of the Orinoco and Amazon River plumes and mesoscale eddies.

IV. Methodology

Experimental Design

Samples were taken along the coast of Puerto Rico and during expeditions throughout the eastern Caribbean basin. From mid September to early October 2007, an expedition was undertaken along the central Caribbean between Puerto Rico and Aruba and then along the northern border of the Caribbean basin and the Gulf of Paria, (Fig. 4). Table 3 gives the stations sampled, their abbreviations, longitude/latitude, salinity values and respective distance from the river mouth.

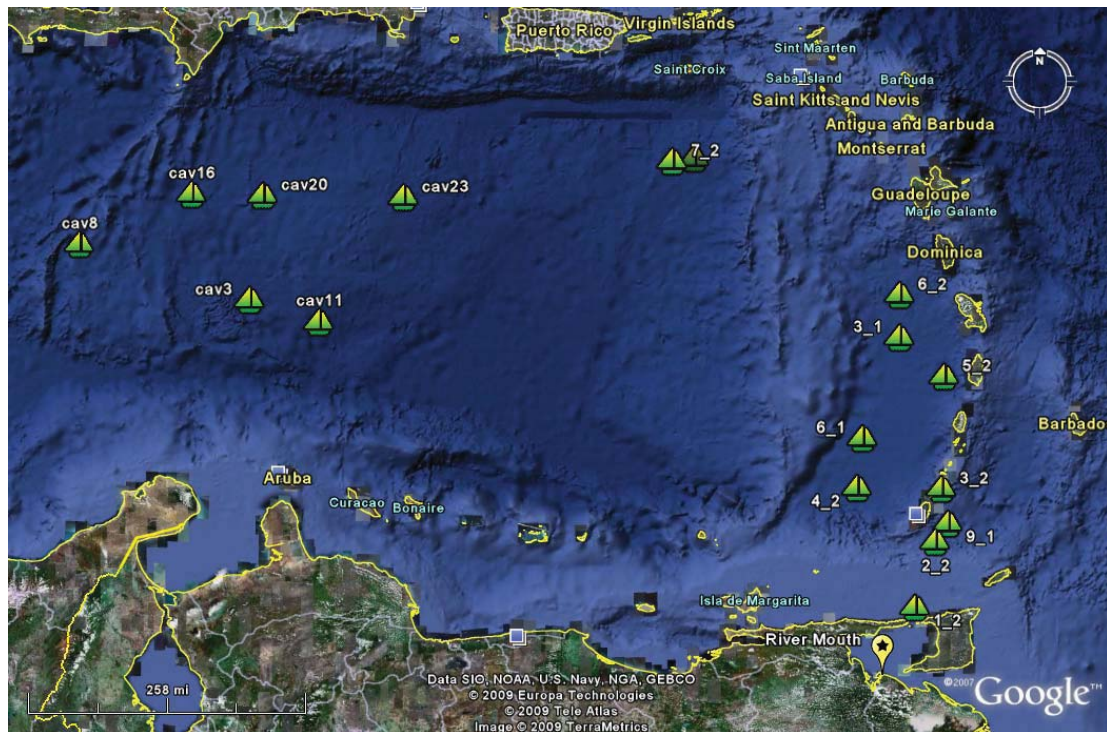


Figure 4. Cruise track. Image obtained from Google Earth. Boats indicate stations, star indicates river mouth of the Orinoco River.

Table 3. Dates, Coordinates (decimal degrees), salinity values and respective abbreviations for stations sampled.

Date	Latitude	Longitude	Distance from River Mouth (km)	Salinity	Abbreviation
Aug 29 2006	14.50067	-70.50	1035.44	35.536	Cav3
Aug 29 2006	15.159	-72.87	1289.48	35.309	Cav8
Aug 29 2006	14.24367	-69.57	935.01	34.855	Cav11
Sep 06 2006	15.83217	-71.34	1196.19	35.615	Cav16
Sep 06 2006	15.82867	-70.37	1107.77	35.731	Cav20
Sep 07 2006	15.834	-68.50	953.33	35.223	Cav23
Sep 19 2006	16.35667	-64.7033	794.32	34.929	2 1
Sep 20 2006	14.10133	-62.0000	495.66	33.279	3 1
Sep 21 2006	12.83148	-62.5015	353.37	32.524	6 1
Sep 22 2006	11.71667	-61.35	249.69	30.169	9 1
Sep 26 2006	10.65	-61.7833	124.30	23.506	1 2
Sep 27 2006	11.48833	-61.52	217.75	31.916	2 2
Sep 27 2006	12.16833	-61.44	296.26	35.035	3 2
Sep 28 2006	12.195	-62.5733	279.68	32.931	4 2
Sep 28 2006	13.60167	-61.3967	441.33	34.145	5 2
Sep 28 2006	14.64167	-61.9883	547.97	33.281	6 2
Sep 28 2006	16.32833	-64.9883	781.45	34.935	7 2

Seawater Collection.

Near-surface and sub-surface waters (depth) and deep chlorophyll maxima (DCM) waters were sampled. The depth of the DCM varied with location but ranged from 17-87 m. Sampling was performed by collecting 10 to 20 L of seawater using Niskin-type PTFE-lined oceanographic sampling bottles. To obtain phytoplankton size fractions, the seawater was filtered sequentially through 20.0, 2.0 and 0.2 μm 47 mm polycarbonate filters. Volume of seawater filtered through each filter varied depending on turbidity and filter capacity. At times it was necessary to use several filters, as the filters clogged and filtration capacity decreased. This was especially true for the 2.0 and 0.2 μm fractions but no less than 8.0 L and no more than 20.0 L were filtered for each analysis. Following filtration, filters were folded in aluminum foil, placed in cryotubes, stored in liquid nitrogen and then transferred to a deep freezer set to -90°C upon returning from the expedition until time of analysis.

Samples were also filtered using Whatman GF/F filters. This was done for three reasons. The first was to ensure a sample backup in case fraction filtration proved insufficient. Second, to obtain a general overview of the pigments present in a bulk filtration and finally to corroborate the findings in the fractionated samples.

Phytoplankton Extraction.

The frozen filters were removed from their foil wrappings, cut into small pieces under dim light, placed in 6 mL glass vials and soaked with approximately 2 mL HPLC grade 90% acetone. Vials were covered with aluminum foil to protect from light. Samples were extracted overnight for 24 hours at 5°C. After the overnight extraction the contents in the vials were quantitatively transferred to a glass grinding tube and mechanically grinded until a slurry was formed. For the samples filtered through polycarbonate filters, a 25 mm GF/F filter was added to the glass grinding tube to aid in disruption of phytoplankton cells in the sample. To prevent degradation of sample from light and heat during grinding, the glass tubes were wrapped in aluminum foil and submerged in an ice bath. After grinding, the contents were quantitatively transferred to a glass microanalysis vacuum filter and the contents were filtered through 25 mm GF/F filters. The filtrate was then quantitatively transferred to a 10 mL measuring cylinder to determine the volume of extract. For samples that were injected into the HPLC using the Waters autosampler, filtrates were then transferred to 4 mL glass amber auto sampler vials and kept at -10° C until analysis by HPLC, usually within the next 4 hours. Otherwise, samples injected into the HPLC via manual injection were transferred back to their 6 mL vials and kept at -10° C until analyzed.

Instrumental Analysis.

Water column properties at sampling stations were characterized using SeaBird Electronics (SBE25) conductivity-temperature-pressure probes and photosynthetic active radiation (PAR) sensors (Biospherical Laboratories). Practical salinity (S) and depth were computed from the primary data using the SBE-provided algorithms. Vertical diffuse attenuation coefficients for PAR (K_d PAR) were obtained from the PAR profiles using exponential fits to the smoothed data.

Extracted samples were analyzed for photosynthetic pigment content on a high pressure liquid chromatograph (HPLC) using a diode array detector (400 nm – 800 nm) for pigment quantification and identification. A modified version developed by graduate student Oswaldo Cárdenas (2006, unpublished) of Jeffery et al. (1997) pigment analysis protocol was used. The full pigment chromatogram was monitored at 435 nm. Pigment identification and pigment concentration were determined using peak maximum, band ratio, peak area and extinction coefficients of the pigment absorption spectrum as described by Barlow et al. (1993) and Cárdenas (unpublished). Table 4 gives chromatographic conditions and table 5 shows the mobile phase parameters that were used.

Table 4. Parameter values used for the HPLC

Parameter	Value
Stationary phase	C-18
Column length	3.9 x 150 mm
Column i.d.	Waters W11501T 046
Mobile Phase	
Solvent A: MeOH/H ₂ O	50:50
Solvent B: MeOH/Acetate, pH 7.2	90:10
Solvent C: Acetonitrile/ H ₂ O	90:10
Solvent D: Ethyl Acetate	
Total Time	30 min

Table 5. Mobile phase parameters used for the HPLC

Time (min)	Flow Rate (mL/min)	Mobile Phase
0-4 min	1 mL/ min	100% B
4.0 – 5.5 min	1.5 mL/min	100% C
18.0 min	1.8 mL/min	20% C, 80% D
21.0 min	1.0 mL/min	100% C
24.0 – 29.0 min	1.0 mL/min	100% B

Solvents were degassed using HPLC grade helium gas for 5 minutes. Samples were injected using either an autosampler with injection volume set to 250 – 500 μ L, depending on sample concentration, or manual injection into a 500 μ L loop.

Materials and instrumentation.

For extractions and HPLC analysis the following HPLC grade solvents were used:

- Methanol (Fisher Scientific), 99.9%
- Acetonitrile (Burdick & Jackson), 99.9%
- Ethyl acetate (Fisher Scientific), 99.9%
- Acetone (Fisher Scientific), 99.6%
- Ammonium acetate (Fisher Scientific) HPLC grade 98.8%

Chlorophyll *a* standard from *Anacystis nidulans* algae (SIGMA) was used to calibrate the HPLC and run system stability tests. Osmonics polycarbonate filters (0.22 µm, 2.0 µm and 20.0 µm pore size), 47 mm diameter were used along with Whatman GF/F 47mm diameter filters. Clear 6 mL glass vials were used for overnight extraction. To protect against light, the vials were wrapped in aluminum foil, samples were filtered using Fisher brand glass microanalysis vacuum filter holders and 25mm GF/F filters to remove particulates from extract solution.

A Glas-Col Homogenizer 333 rpm was used for grinding filtered samples extracted in acetone. To measure pH of mobile phase B, a Corning pH/ion analyzer model 350 was used. For chromatography, a Shimadzu HPLC/Diode Array system, (HPLC Model LC-10AT, Diode Array Detector Model SPD-M10AT) was used. Either a Millipore Waters model 712 WISP autosampler, or a 500 µL Hamilton 80865 glass syringe and loop injector were used in conjunction with the HPLC/DAD sample injection.

Quality Control

All HPLC lines were tested for leaks using a soap solution. An evaluation of equipment was done by performing a system blank before each batch run. Calibration was performed using the well characterized Chl*a* peak. This compound has a specific absorption coefficient of 87.67 mg⁻¹cm⁻¹ at 664 nm (Jeffery et al., 1997).

The piston and glass tube of the homogenizer was washed before each batch set was individually grinded using soap and water followed by distilled water and acetone. Between sample grindings, the piston and glass tube was rinsed with acetone. In order to eliminate possible interferences, glassware was cleaned with soap and tap water, followed by an acid

wash and rinsed three times with distilled water. Finally glassware was rinsed with acetone and air dried. Prior to any analysis a column blank was performed to determine the conditions of the column. If conditions required, blanks were continued to be run to ensure the good conditions of the system.

V. Results

Physical Characteristics

In the late fall, near surface water mass properties in the Eastern Caribbean are significantly influenced by continental runoff through the Orinoco River plume (Corredor and Morell 2001). In our work, we found that the salinity ranged from 23.5 in near-field of the river mouth to 35.7 in the far-field at a distance of 1,100 km from the river mouth (Fig. 5). K_d PAR values along this gradient varied between 0.063 and 0.453 m^{-1} (Fig. 5) and increase proportionally with $Chl a$ values as we approach the river plume (Fig. 7). The depth of the deep chlorophyll maximum (DCM) in turn decreased along this gradient until the DCM ceased to exist at distances less than 200 km away from the river mouth (Fig. 6). Salinity and diffuse light attenuation vary widely and consistently along the river plume. Accordingly we use these parameters as proxies for river influence.

Phytoplankton communities in potential eddy fields were also sampled. Sea Surface Height anomaly (SSHA), $Chl a$ values and current flow as depicted in the Colorado Center for Astrodynamics Research-CCAR Satellite Oceanography web page, indicate that stations 16 and 20 were within a cyclonic region while stations 3, 8, 11 and 23 were within an anticyclonic region (Fig. 8).

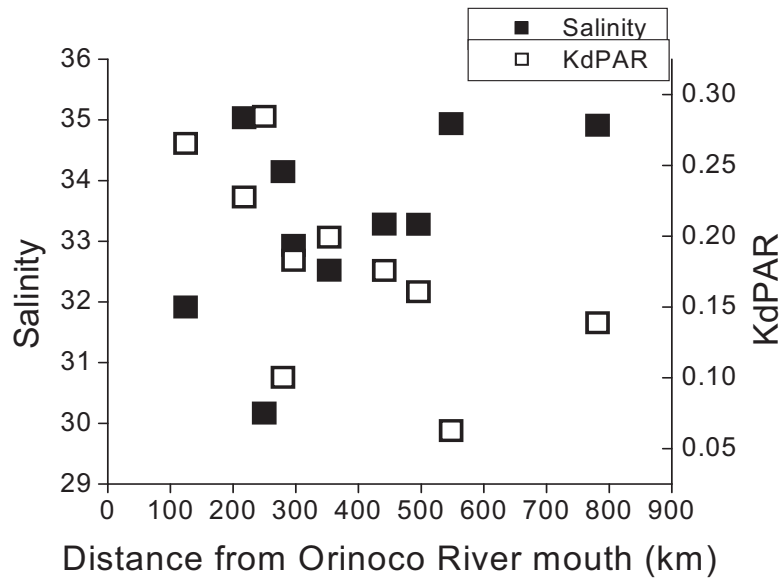


Figure 5. Near-surface salinity and KdPAR values with respect to distance of the Orinoco River Plume.

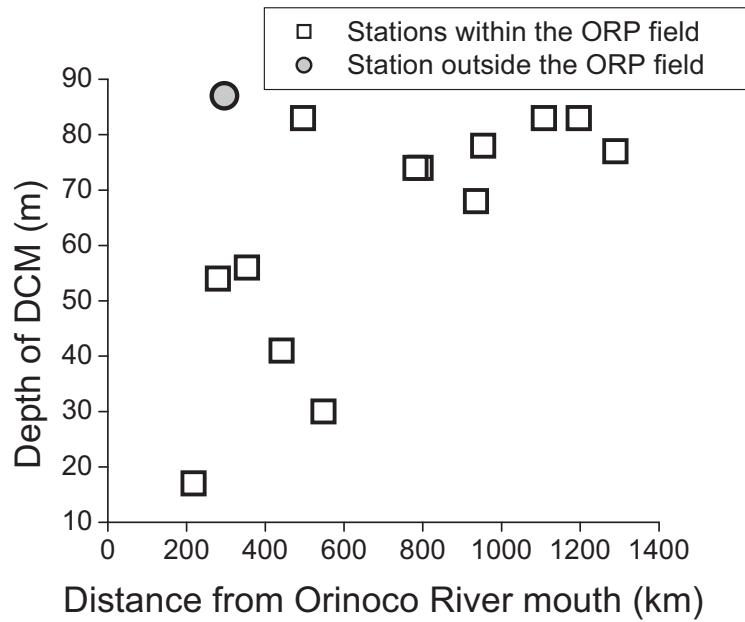


Figure 6. Depth of the deep chlorophyll maximum (DCM) along the distance gradient of the Orinoco River Plume (ORP).

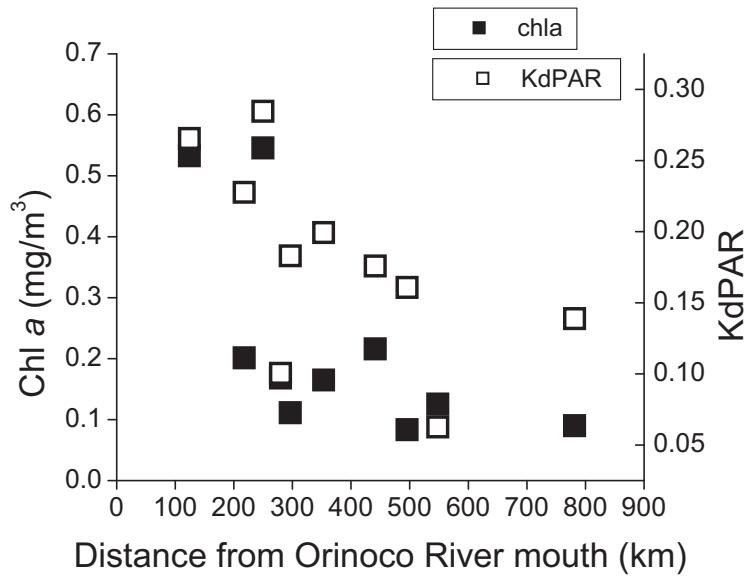


Figure 7. Spatial distribution of KdPAR and near surface Chl a concentrations along the river plume.

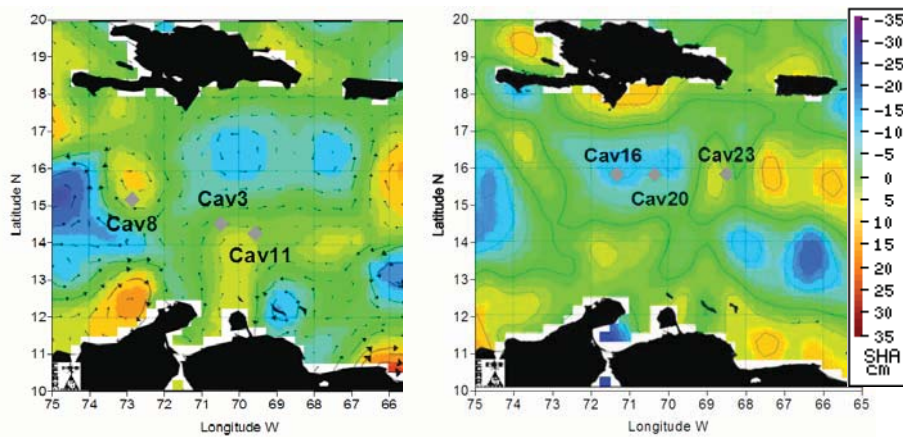


Figure 8. Sea surface height anomaly (SSHA) for stations Cav3, Cav8, Cav11, Cav16, Cav20 and Cav23. Negative sea surface height anomaly is indicated by blue regions.

(<http://argo.colorado.edu/~realtime/modis/>)

Phytoplankton pigment distribution

Photosynthetic pigments identified using GF/F extraction during the course of this study were: Chlorophyll's *c1* and *c3*, Divinyl Chlorophylls *a* and *b*, phytillated Chl*c*, 19'-BF, 19'-HF, fucoxanthin, diadinoxanthin, alloxanthin, zeaxanthin and $\beta\epsilon$ - and $\beta\beta$ -carotene. Surface concentrations of fucoxanthin and Chl*b* increased as we approached the near field of the river plume while 19'-HF and 19'-BF remained relatively unchanged throughout the salinity gradient. Zeaxanthin also increased as we moved from far field to mid field, however, within the near-field concentrations dropped (Fig. 9).

Pigment distribution within the DCM was similar to that of the surface samples. At the DCM, fucoxanthin and zeaxanthin increase as we approached the near field of the river plume. 19'-HF was relatively unchanged while 19'-BF and Chl*b* were at higher concentrations in the mid and far fields (Fig. 10). Response of surface pigment concentration to K_d PAR showed similar results as with surface salinity (Fig. 11).

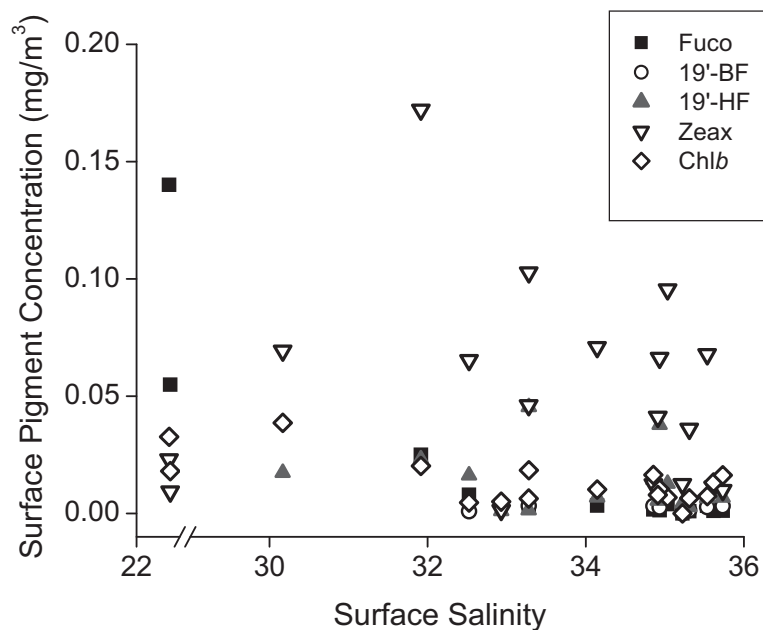


Figure 9. Surface pigment concentrations and distribution along the salinity gradient.

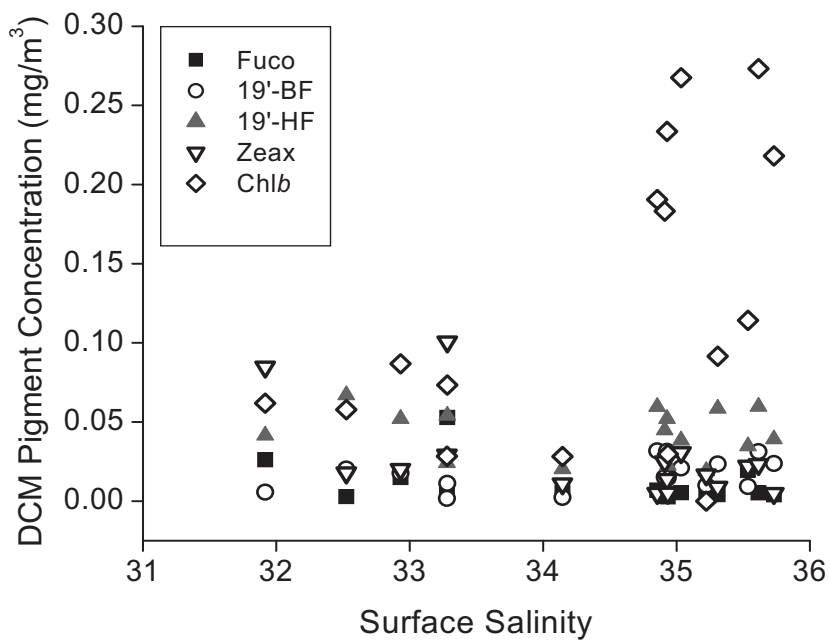


Figure 10. DCM pigment concentrations and distribution in relation to the surface salinity gradient.

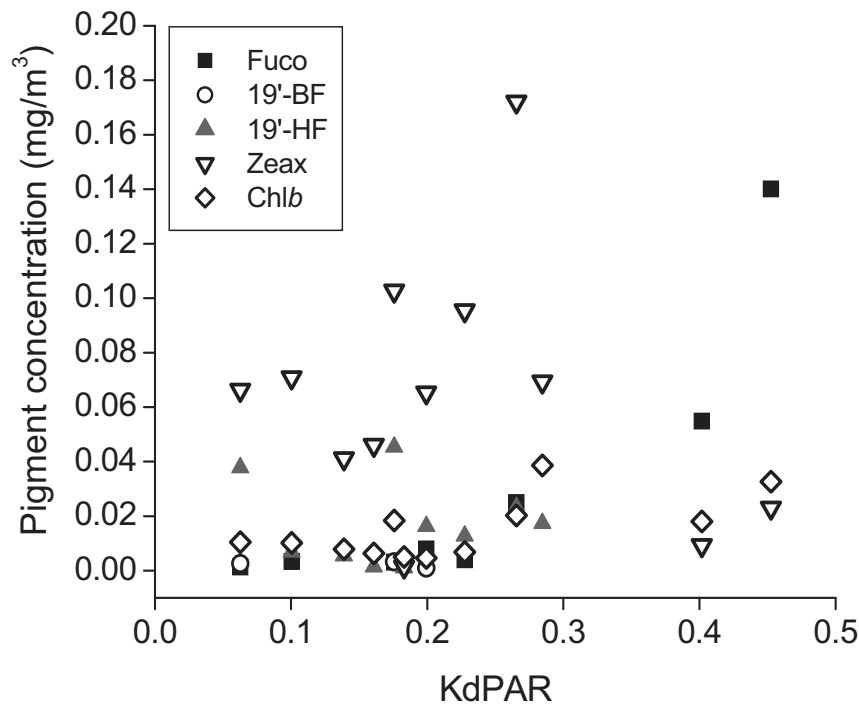


Figure 11. Pigment distribution along the KdPAR gradient.

In the oceanic eddy field, the general abundance of pigments within the DCM appears to increase around the edge of the anticyclone eddies, as observed by Martin et al. (2001, 2003). The cyclonic eddy showed greatest pigment abundance at its center. Overall biomass in terms of *Chla* concentrations was greater at stations 16 and 20 within the cyclonic eddy than at station 23 which was within an anti-cyclonic eddy. However, comparative analysis of stations 16 and 20 to the anticyclone stations of 3, 8 and 11, shows that *Chla* concentrations were higher at the later stations (Fig. 12 and 13). No relationship was observed between isopycnal displacement and depth of DCM in either the cyclone or anticyclone eddies.

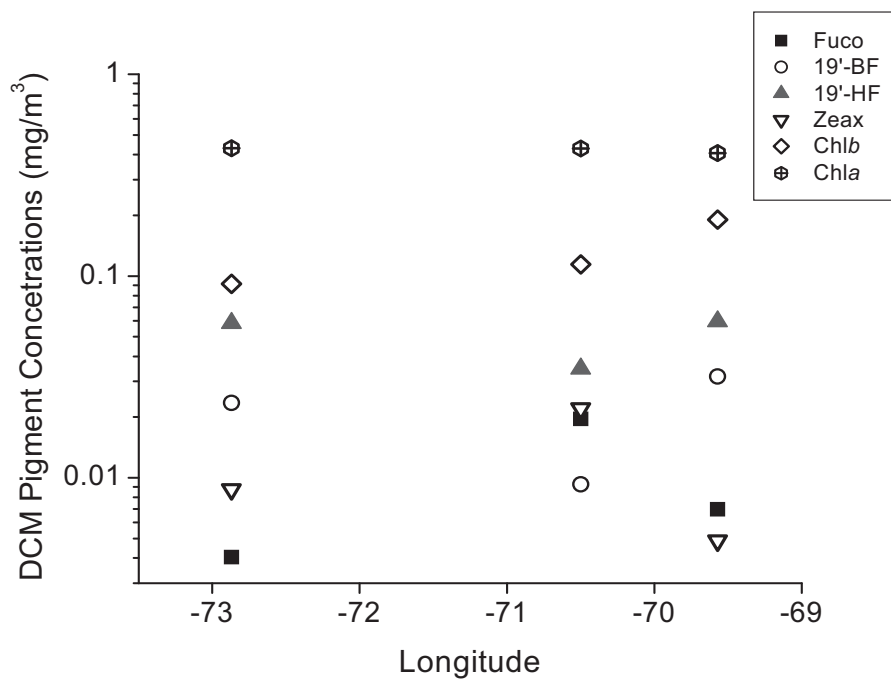


Figure 12. DCM pigment concentration for stations Cav3, Cav8, and Cav11.

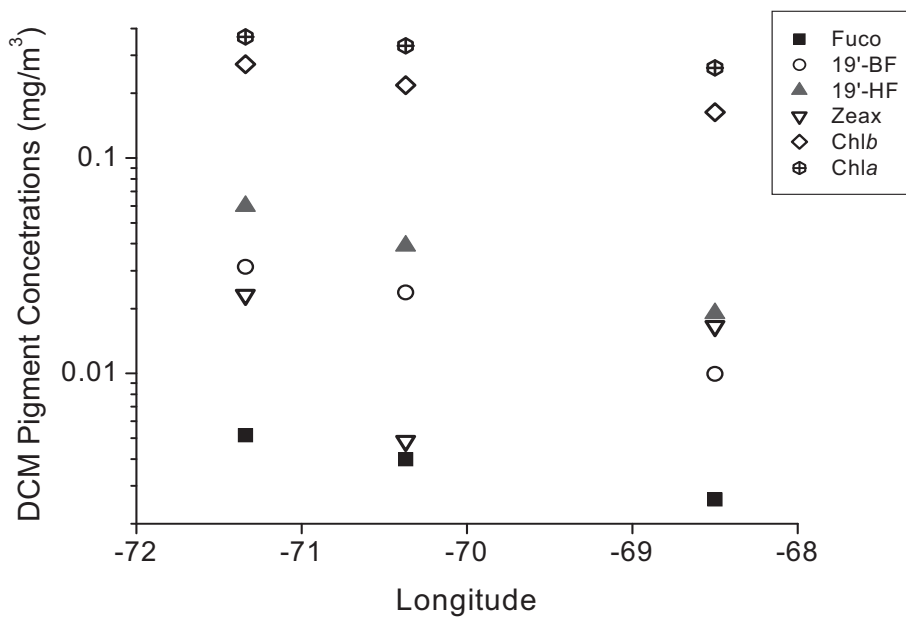


Figure 13. DCM pigment concentration for stations Cav16, Cav20 and Cav23.

Phytoplankton community structure as inferred from bulk sample pigment composition

Influence of the River Plume.

Community size structure was estimated from the five diagnostic pigments discussed in Table 2. With the exception of 19'-BF all pigments in both surface and DCM waters showed a general increase in concentration, and hence community biomass, along the plume gradient towards the river mouth. Surface zeaxanthin, a marker pigment of picoplanktonic cyanobacteria and prochlorophytes, ranged from approximately 0.01 to 0.17 mg/m³ and steadily increased from the high salinity regions to the mid salinities (36 to 31 respectively) as we approached the influence of the plume. However, zeaxanthin concentration, and hence, cyanobacteria and prochlorophyte populations dropped abruptly when salinity reached 24 within the near-field of the plume.

In near-field surface waters, detection of 19'-BF was minimal whereas 19'-HF and Chl***b*** were found to be in a greater concentration than fucoxanthin in both the mid and far-field of the river plume indicating a dominance of picoplanktonic prochlorophytes and cyanobacteria along with nanoplanktonic chromophytes in these regions. Chl***b*** and 19'-HF were at relatively similar proportions within the mid and far-fields. However, in the near-field a shift in community structure was apparent by the increase of fucoxanthin concentrations, which is representative of diatom populations.

Results from DCM samples mirrored the surface samples with the exception of having a more marked dominance of picoplankton over nanoplankton in the mid and

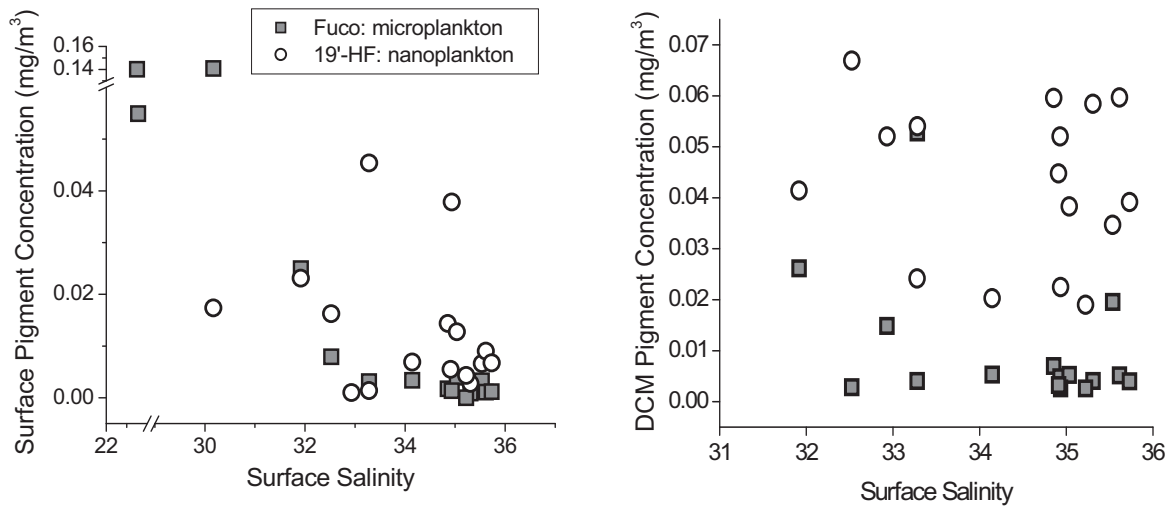


Figure 14. Distribution of taxonomic pigments along surface salinity gradient. Microplankton populations are represented by fucoxanthin while nanoplankton populations are represented by 19'-HF.

far-fields. Figures 14, 15 and 16 show the comparison and distribution of the phytoplanktonic size structure identified based on pigment taxonomy in surface and DCM waters as we approached the river plume.

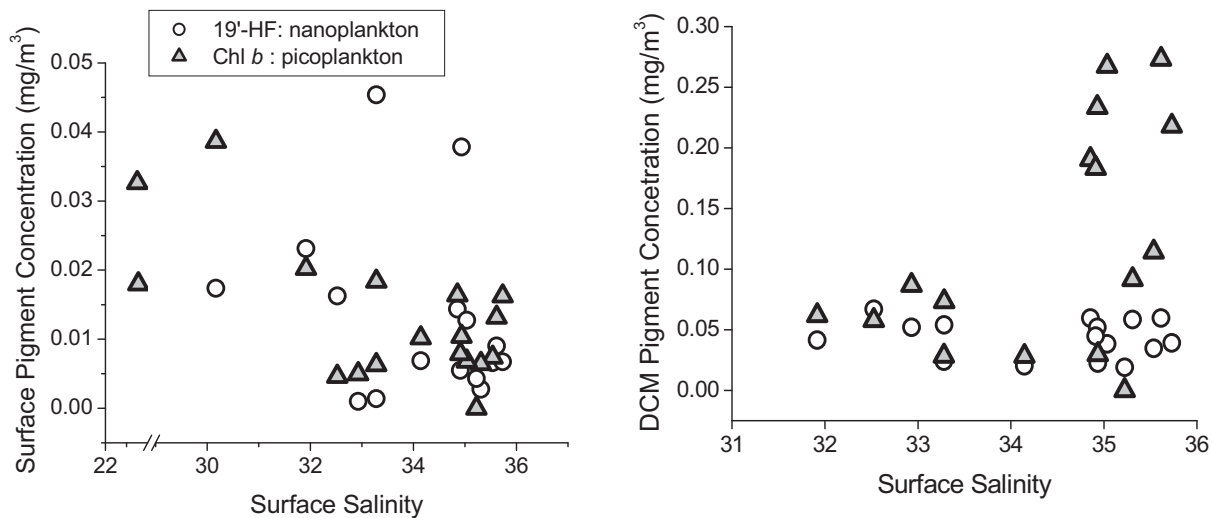


Figure 15. Distribution of taxonomic pigments along surface salinity gradient. Nanoplankton populations are represented by 19'-HF while picoplankton populations are represented by Chl *b*.

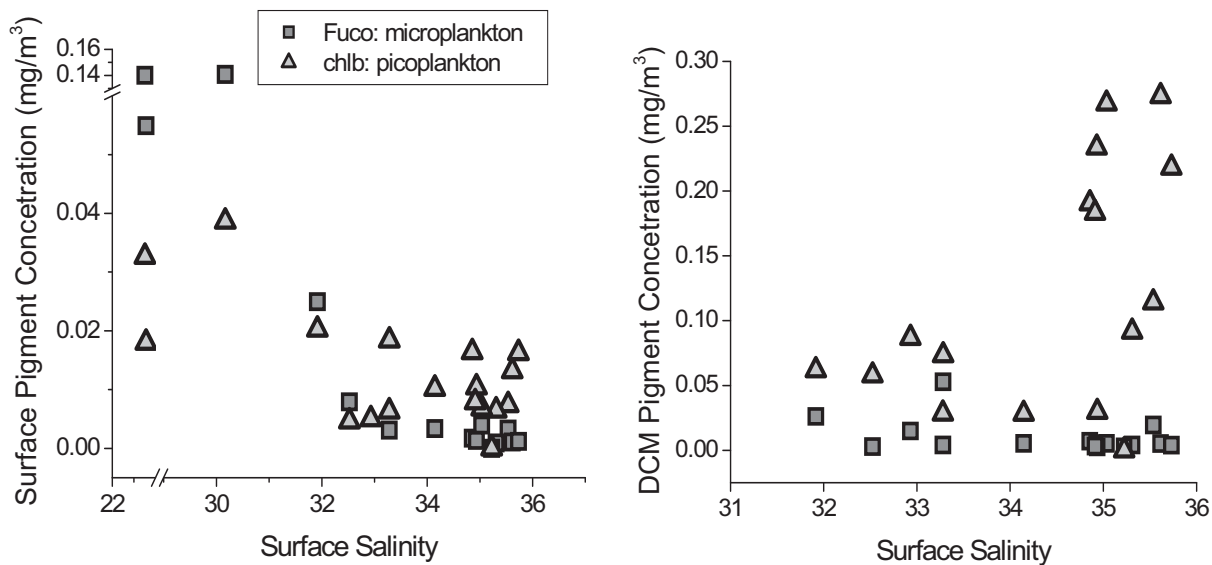


Figure 16. Distribution of taxonomic pigments along surface salinity gradient. Microplankton populations are represented by fucoxanthin while picoplankton populations are represented by Chl *b*.

Influence of Meso-Scale Eddies

Community composition at the DCM in both the cyclonic and anticyclonic eddies showed little variability. Based on pigment taxonomy and assuming each class represents its putative size structure, populations were dominated mostly by picoplanktonic cyanobacteria and prochlorophytes, followed by nanoplanktonic chromophytes and finally microplanktonic diatoms.

Between stations 3, 8 and 11 diatom populations and cyanobacteria along with prochlorophyte populations were at their highest in station 8 while chromophyte populations were lowest. Zeaxanthin concentrations were also highest at station 8, however at station 11 while *Chl b* concentration was at its highest, zeaxanthin concentration was at its lowest. Among stations 16, 20 and 23 pigment concentrations steadily decreased from station 16 to 23, indicating a decrease in all phytoplankton classes as we move eastward across the cyclonic eddy center and into the anticyclonic eddy region (see Fig. 12 and 13).

Phytoplankton size distribution as derived from sequential fractionated filtration.

Surface and DCM samples taken throughout this expedition were fractionated in order to characterize the actual size fraction composition and distribution of the diagnostic pigments within these size classes. Results show, in the majority of the cases, that pigments commonly used for size classification appear throughout the size fractions (Fig. 17 and 18). Tables 6 and 7 show the proportional distribution of the five diagnostic pigments throughout the size spectrum.

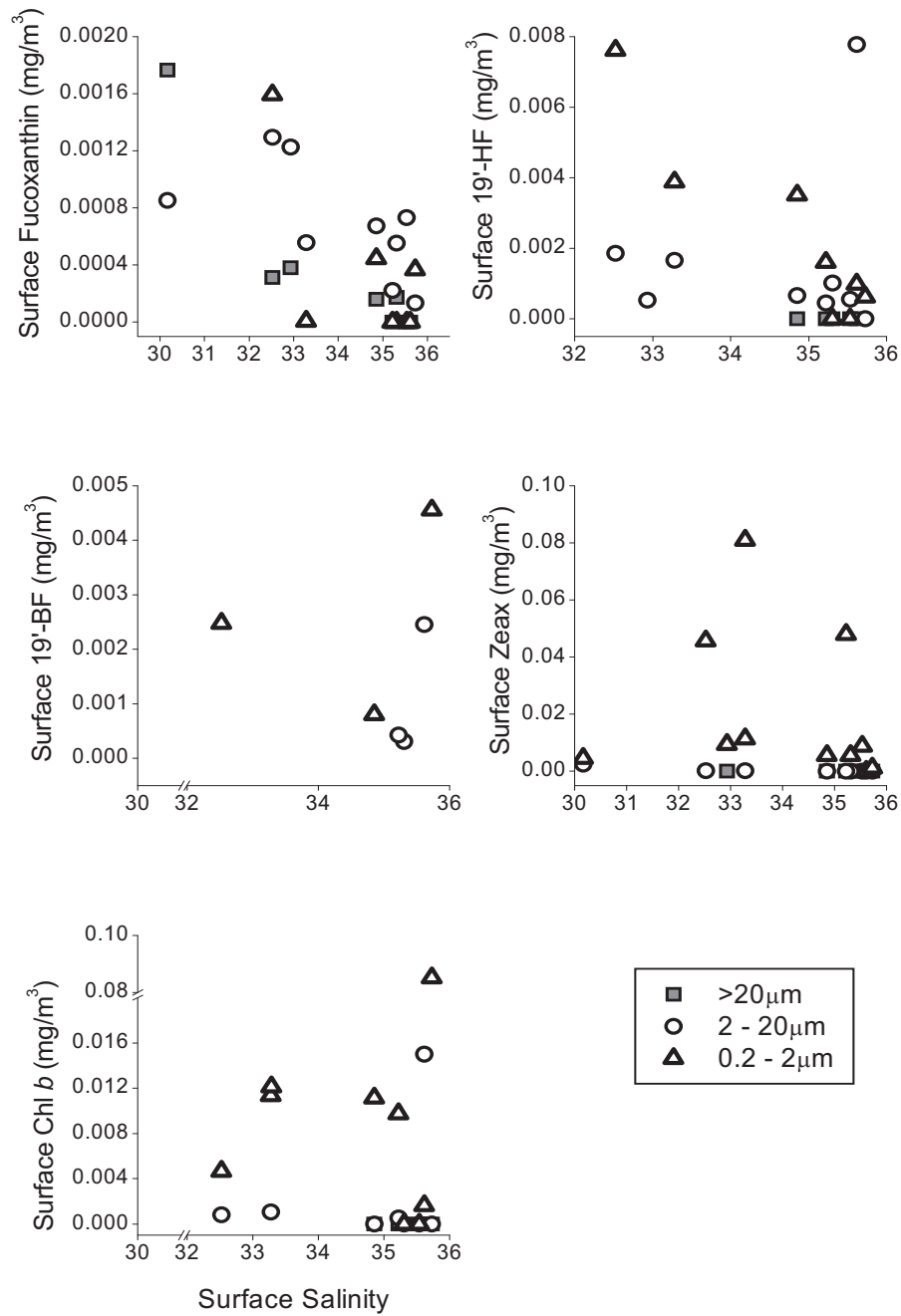


Figure 17. Distribution of surface taxonomic pigment concentration within the size fraction along the surface salinity gradient.

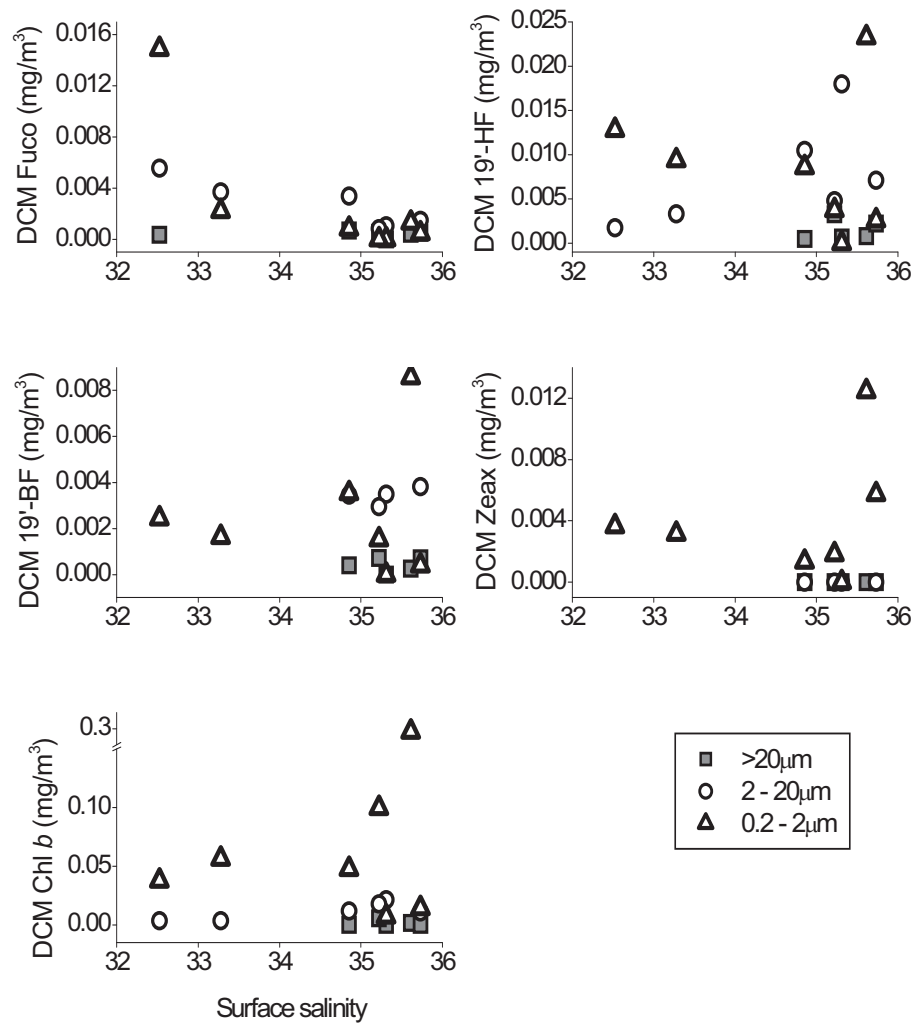


Figure 18. Distribution of DCM taxonomic pigment concentration within the size fraction along the surface salinity gradient.

Table 6. Proportional distribution of surface taxonomic pigments within the size fractions.

	$\geq 20 \mu\text{m}$	$20 - 2 \mu\text{m}$	$2 - 0.2 \mu\text{m}$
Fuco	26	53	21
19'-BF	0	50	50
19'-HF	0	57	43
Zeax	7	21	71
Chl <i>b</i>	0	40	60

Table 7. Proportional distribution of DCM taxonomic pigments within the size fractions.

	$\geq 20 \mu\text{m}$	$20 - 2 \mu\text{m}$	$2 - 0.2 \mu\text{m}$
Fuco	31	38	31
19'-BF	29	29	43
19'-HF	29	35	35
Zeax	0	0	100
Chl <i>b</i>	13	40	47

VI. Discussion

Influence of meso-scale phenomena on phytoplankton population distribution.

Open ocean studies have found nano and picoplankton to comprise approximately 45% each of total biomass, giving way to the larger microplankton populations in the more eutrophic regions with total biomass size classes distribution of 75% microplankton, 21 and 4% nanoplankton and picoplankton, respectively (Uitz et al., 2006). In the oligotrophic waters of the North Atlantic HPLC pigment analysis (Andersen et al., 1996) indicates that phytoplankton communities are comprised mainly of nano (chromophytes and prymnesiophytes) and picoplankton (cyanobacteria, prochlorophytes and green flagellates. Silva et al. (2008) found a dominance of micro and nanoplankton within Lisbon Bay while in the Mediterranean region nanoplankton tend to be more dominant except during blooms, in which case the microplankton fraction dominate (Vidussi et al., 2001; Barlow et al., 1993; Bustillos et al., 1995).

Yet there have been studies to show a different pattern in phytoplankton population where picoplankton were found to dominate. Marañón et al. (2001) reported fractionated Chl a measurements to be dominated by picoplankton in a range of environments which included temperate, subtropical, equatorial and upwelling waters. His results demonstrate that picoplanktonic abundance is not confined to oligotrophic waters and in fact picoplankton play an important role in the global carbon budget.

The impacts mesoscale phenomena have on phytoplankton community structure and population distribution was studied and investigated. In this section of the study bulk samples were collected using GF/F filters in the oligotrophic Caribbean region under the

influence of mesoscale eddies and along the eastern Caribbean down to the Gulf of Paria where the Orinoco River entrains.

Upwelling of nutrients such as nitrate, nitrite, phosphates and silicates in cyclonic and anticyclonic eddies brings about larger micro and nanoplanktonic populations bloom (Vaillancourt et al., 2003; Bidigare et al., 2003; Williams et al., 1998; Mcguillicuddy et al., 2007, Brown et al., 2008, Martin et al., 2001, Rodriguez et al., 2003, Whitney et al., 2002). As a result, those phytoplankton with hard silica and calcite walls have an important impact on carbon transported to deep waters by the sinking of aging cells and fecal pellets (Vaillancourt et al., 2003).

Although differences between cyclonic and anticyclonic regions were minimal, in this study a slight increase in abundance of pico and nanoplankton is noted within the cyclonic regions. Overall pigment ratios (with the exception of fucoxanthin) were higher within the cyclones, which is in accord with the findings of Vidussi et al. (2001), who compared biomass proportions within cyclone and anticyclone eddies. At station Cav3, however, a sharp increase in fucoxanthin is observed (Fig. 19). This increase could be an indication of a shearing zone. Shearing zones are produced by eddy-eddy collisions which induce either upwelling or downwelling of the water column. In such cases an increase in nutrient concentration and an accumulation of biomass is observed, respectively. Such eddy-eddy interactions have led to the discovery that possibly the regions of highest primary productivity of an anticyclonic eddy may be found along the edge of the eddy (Lima et al., 2002; López Rosado, 2008).

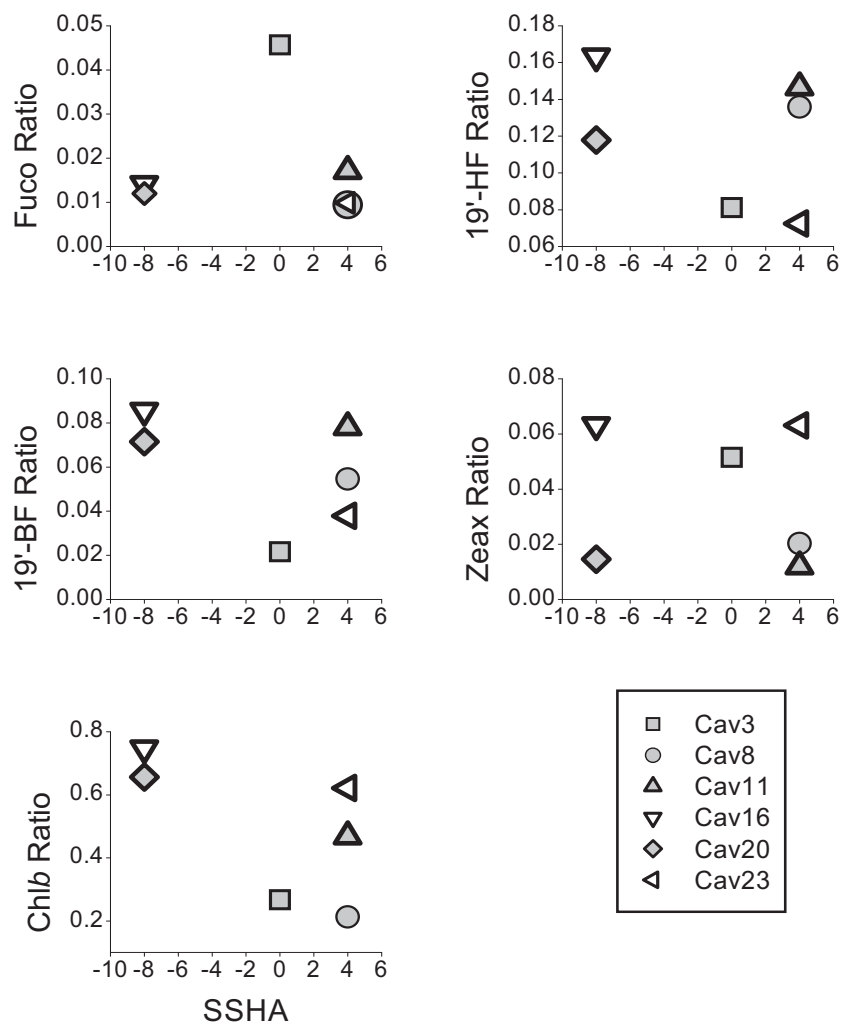


Figure 19. Chemotaxonomic pigment ratios calculated with respect to Chl*a* within the deep chlorophyll maxima (DCM). Sea surface height (SSH) indicates regions of cyclonic and anticyclonic activity.

Near surface salinity constitutes a useful proxy for riverine influence in the Orinoco River plume (Del Castillo et al., 1999; Bidigare et al., 1993). Using ratios of five diagnostic pigments to total Chl*a* of GF/F filtrates we confirm observations of Bidigare et al. that the proportion of 19'-BF and 19'-HF, and Chl *b* and Zeax, marker pigments ascribed to the nano and picoplanktonic classes respectively, show a marked

decrease toward the near-field region of the river plume. Similarly, we observed that fucoxanthin, a microplankton diagnostic pigment ratio increases along the gradient (Fig. 20). DCM samples show similar patterns with the exception of 19'-HF, which did not vary significantly along the plume gradient. As observed by Bidigare et al. (1993) the former is much less abundant at depth in the DCM. There was however a modest increase in the zeaxanthin ratio at the DCM approaching from the high salinity far-field to the near-field. The coincident surface decrease of both zeaxanthin and Chl*b* ratios toward the near-field denotes decreased influence of cyanobacteria. Since zeaxanthin is a known photoprotective pigment produced by eukaryotic taxa as well, the DCM increase could be partially due to a photoprotective response to increased irradiance as the DCM shoals towards the near-field (Fig. 21).

To obtain an additional idea on the overall biomass contribution of size fractions as derived from bulk GF/F filtration the total biomass proportion was determined. Surface biomass proportion (BP) associated with each size class based on pigment taxonomy was calculated using an adaptation of Vidussi's pigment data reduction (Vidussi et al., 2001).

The biomass proportion associated with each size class was calculated as follows:

$$BP_{\text{pico}} = (\text{Zeax} + \text{TChl}b) / DP \quad (1)$$

$$BP_{\text{nano}} = (19'\text{-HF} + 19'\text{-BF}) / DP \quad (2)$$

$$BP_{\text{micro}} = \text{Fuco} / DP \quad (3)$$

Where the diagnostic pigment (DP) is defined as the following:

$$DP = Zeax + TChl\ b + 19'\text{-HF} + 19'\text{-BF} + Fuco \quad (4)$$

For this purpose, far (practical salinity 34.855 to 35.731), mid (32.524 to 34.145) and near (practical 23.506 to 31.916) fields are defined. This analysis indicates that the BP for the micro and pico classes vary little in surface waters within the far and mid-fields, with picoplankton being dominant followed by nanoplankton and finally the microplankton which make a small contribution (Fig. 22). Although the change is small, a slight increase in microplankton biomass is apparent from far-field to mid-field.

However, there is an evident community shift within the near-field where dominant size classes are the pico and micro fractions. The slight increase in picoplanktonic biomass from far-field to mid-field may be due to an increase in river plume borne nutrients. Yet, although picoplankton still remained dominant in the near-field region, its relative biomass proportion decreases while microplankton BP increased significantly.

Contrary to the findings of Bidigare et al. (1993) in the eastern Caribbean, and, in accordance with the findings of Marañón et al. (2001), picoplankton BP in this study consistently exceeded that of nanoplankton (Fig. 22). Moreover, while picoplankton BP only decreased moderately in the near field, nanoplankton BP decreased consistently along the gradient. Increased abundance of *Trichodesmium* and the diatom-symbiont cyanobacterium *Richelia intracellularis* (Corredor, personal communication), both

groups exceeding by far the 20 μm cutoff for microplankton size, may account for the apparent picoplankton BP increase as such organisms are commonly ignored in chemotaxonomic size classification schemes.

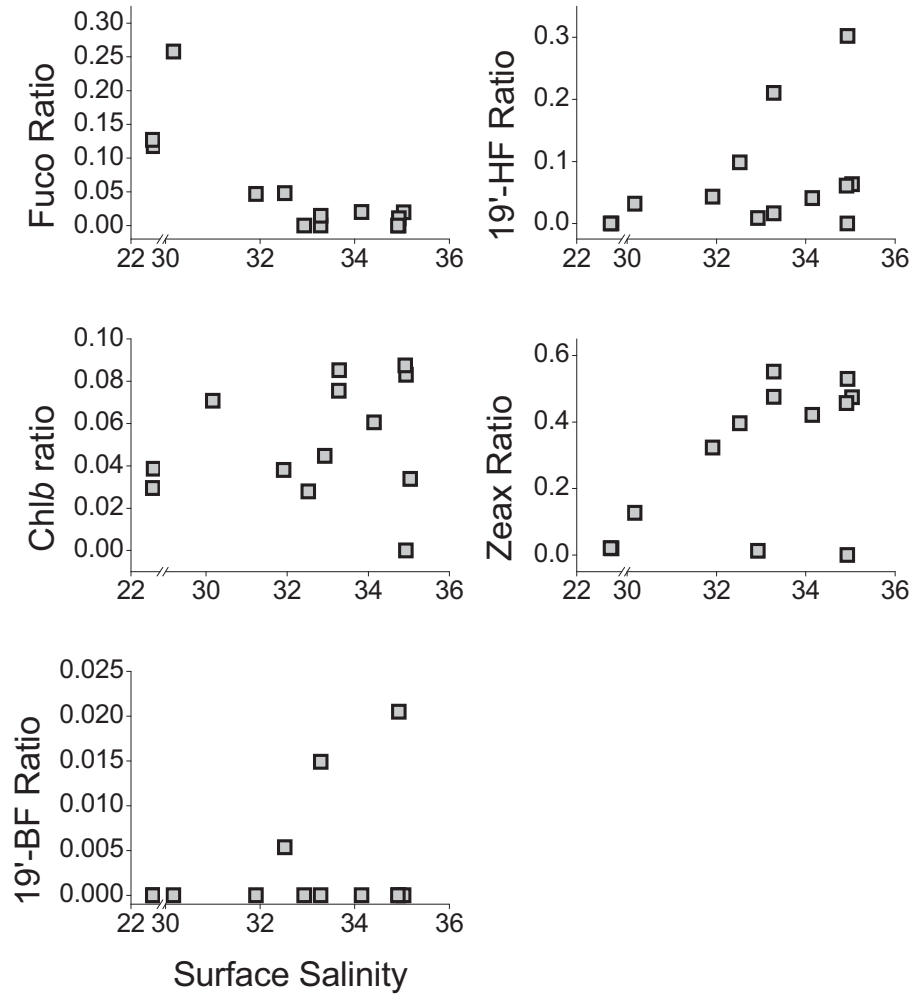


Figure 20. Surface pigment ratios (pigment/ *Chl a*) along the surface salinity gradient.

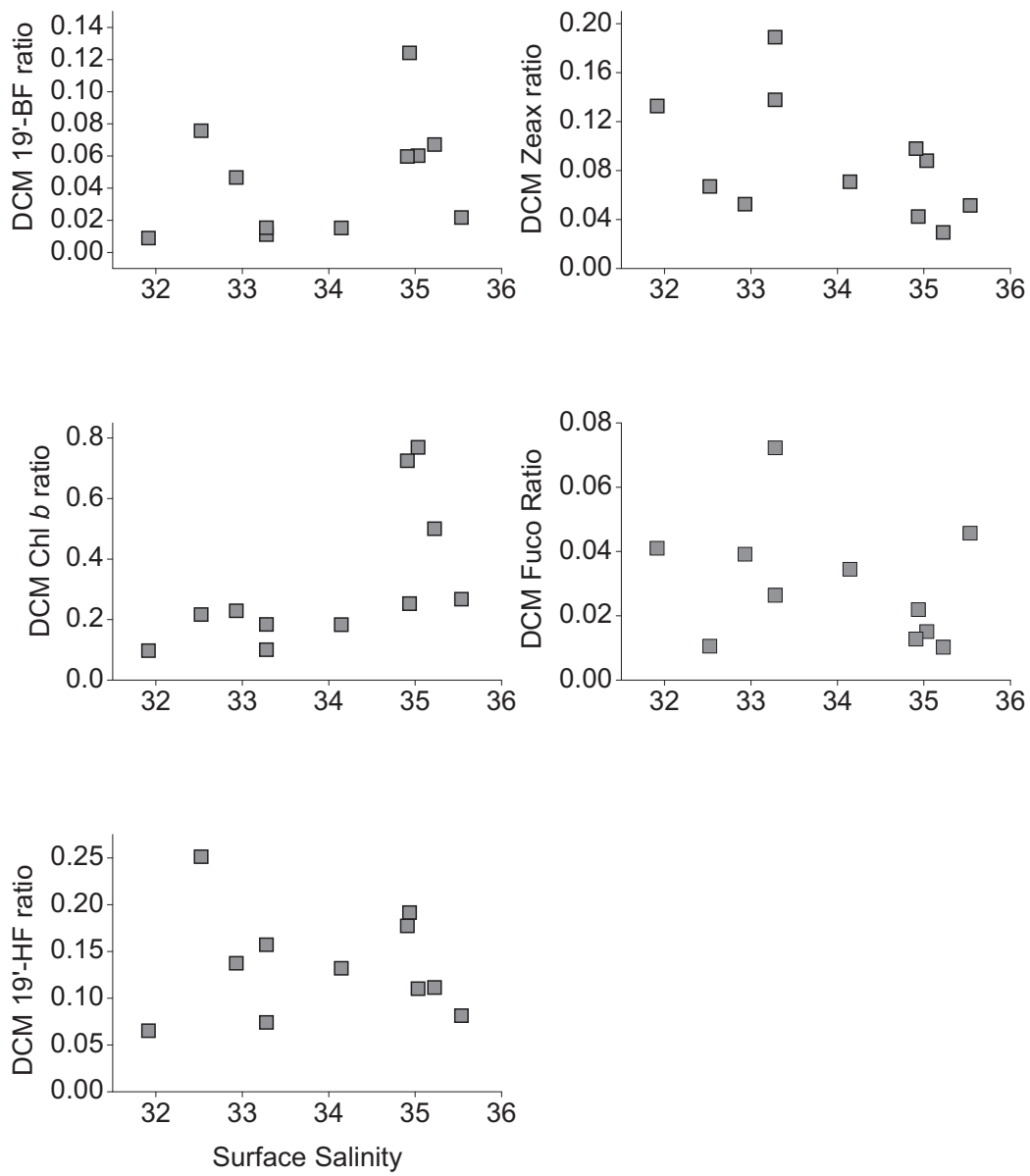


Figure 21. DCM pigment ratios along the surface salinity gradient.

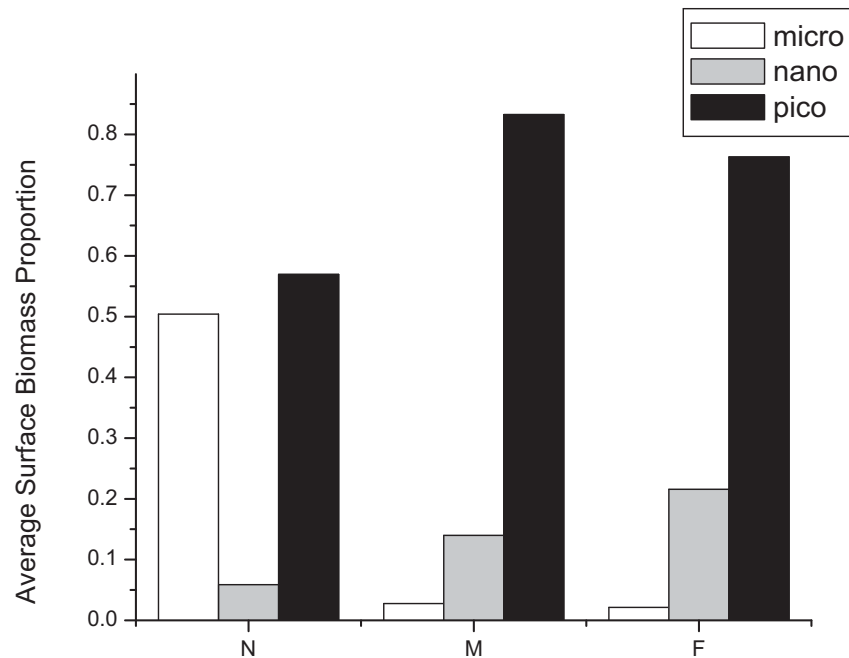


Figure 22. Surface biomass proportion. N = Near-field, M = Mid-field, F = Far-field

Size fractionation of phytoplankton populations.

As the larger phytoplankton size fractions (canonically >2 and $>20 \mu\text{m}$) more vigorously promote vertical oceanic C flux (Geider, 1988; Rivkin et al., 2002; Lance et al., 2007), understanding the parameters that influence size class distribution is essential in order to understand their role in determining the different carbon pathways of oceanic carbon sequestration. The emerging paradigm is that microplankton ($\geq 20\mu\text{m}$) predominate in eutrophic conditions giving way to nano and picoplankton under oligotrophy.

A commonly used method to infer community composition from size structure, fluorometric Chla analysis following fractionated filtration (Marañón et al., 2001; Lance et al., 2007; Hashihama et al., 2008) can lead to erroneous taxonomic adjudication. Some species can group together to form colonies (eg. *Trichodesmium*) or mats (eg. *Rhizosolenia*), much larger than the individual cells and the cyanophyte *Richelia intracelularis*, common in Caribbean waters is a symbiont of much larger diatoms. Conversely, chemotaxonomy, using diagnostic photosynthetic pigments is a useful tool to assess size class distribution (Roy et al., 2006) but discrepancies in identification of diagnostic pigments for the different classes detract from its general applicability. As microscopic analyses reveal putative “microplanktonic” species within the “nanoplanktonic” size range (Geider 1988; Anderson et al., 1996; Vidussi et al., 2001; Roy et al., 2006) such generalization of size class based on pigment taxonomy can lead to underestimation of the impact of certain size classes on primary production and consequently on carbon drawdown, leading also to overestimation of other phytoplankton classes. Moreover, HPLC analysis using GF/F filters which have pore sizes of 0.7µm can overlook the smallest fraction of the picoplankton present in the sample. Thus, diagnostic pigments, although useful to identify phytoplankton taxa, may not necessarily correspond to phytoplankton size structure.

Sequential filtration using well defined pore size membrane filters followed by HPLC analysis provides a clearer view of the relationship between pigment-based chemotaxonomic composition and phytoplankton community size structure despite drawbacks, such as the large volume of water and time needed to filter samples among others (Silva et al., 2008; Craig 1986). Rodriguez et al. (2003) for example found 19'-BF,

19'-HF and fucoxanthin within the picoplanktonic size fraction along with Chl*b* and zeaxanthin in the nano and micro-fraction size range. The presence of diatoms in the nano-fraction and dinoflagellates in the pico-nano fractions was corroborated by cell count using an inverted microscope.

Regional information on size structure of phytoplanktonic communities is scarce and little is known regarding pigment content or size class composition of phytoplankton communities in the eastern Caribbean other than the early work of Malone (1971) who reported 85% of the Chl *a* associated with the >20 μm size fraction in more oligotrophic waters (except in cases when colonial cyanobacteria were present) and of Bidigare et al. (1993) who, based on HPLC analysis of GF/F filtrates, reported increased abundance of pigments associated to nano and microplankton in surface waters influenced by the ORP.

In this study, analysis of fractionated samples taken from all far field stations and two mid-field stations (St.4_2 and St. 6_2) revealed that a significant proportion of specific taxonomic pigments can be found distributed among the size ranges. The operational classes - picoplankton, nanoplankton and microplankton - when characterized on the basis of taxonomic marker pigments found in the different filter fractions were all found distributed among the 0.2, 2.0 and 20 μm size fractions (Fig. 23, 24 and 25).

The microplanktonic marker pigment fucoxanthin was found to be more abundant in the nano-fraction in surface samples, with only trace amounts found in the pico-fraction. DCM samples exhibited an almost even distribution of fucoxanthin within the three size fractions. In high salinity oligotrophic surface waters fucoxanthin was mostly found in the nano-fraction followed by the micro-fraction with a small percent in the

pico-fraction. Low salinity waters influenced by the ORP revealed a predominance of fucoxanthin in the micro-fraction, followed by the nano and then the pico-fractions.

Marker pigments 19'-HF and 19'-BF commonly associated to the nanoplankton fraction were abundant in the nano and pico-fraction in surface samples, however DCM samples revealed a proportion of these nanoplanktonic marker pigments in the micro-fraction. This proportion is found in the high salinity oligotrophic waters. This could be a result of zooplankton grazing on nanoplankton, which were consequently caught on the 20 μ m filter. However this would have to be corroborated with the presence of pheophorbides and/or pheophytins, which could not be clearly detected in the analysis. On the other hand, picoplanktonic *Prochlorococcus* can be found in lengths up to 1.6 μ m (Jeffery et al., 1997) and could subsequently be caught on the 2 μ m filter as filter capacity decreases with the increased capture of particles.

The picoplanktonic marker pigments zeaxanthin and Chl***b*** were mostly found in the pico-fraction. Only one sample revealed trace amounts of zeaxanthin in the micro-fraction. All others showed zeaxanthin to be within the pico-fraction. A fraction of Chl***b*** in the oligotrophic waters, however, was found in the nano-fraction. Oligotrophic DCM samples revealed a small amount of Chl***b*** also in the micro-fractions.

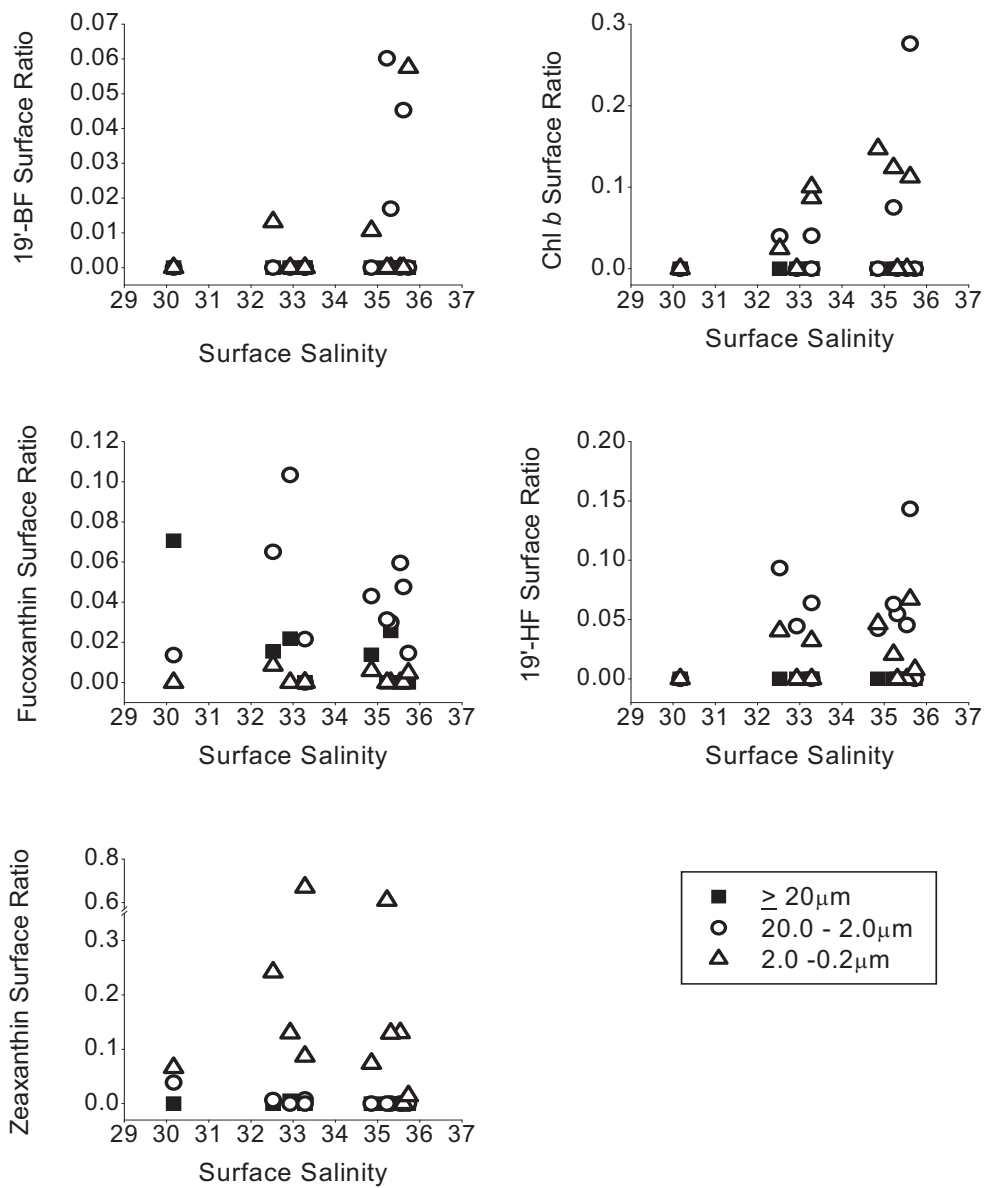


Figure 23. Ratios of surface sample of taxonomic marker pigments to Chl *a* within the size fraction.

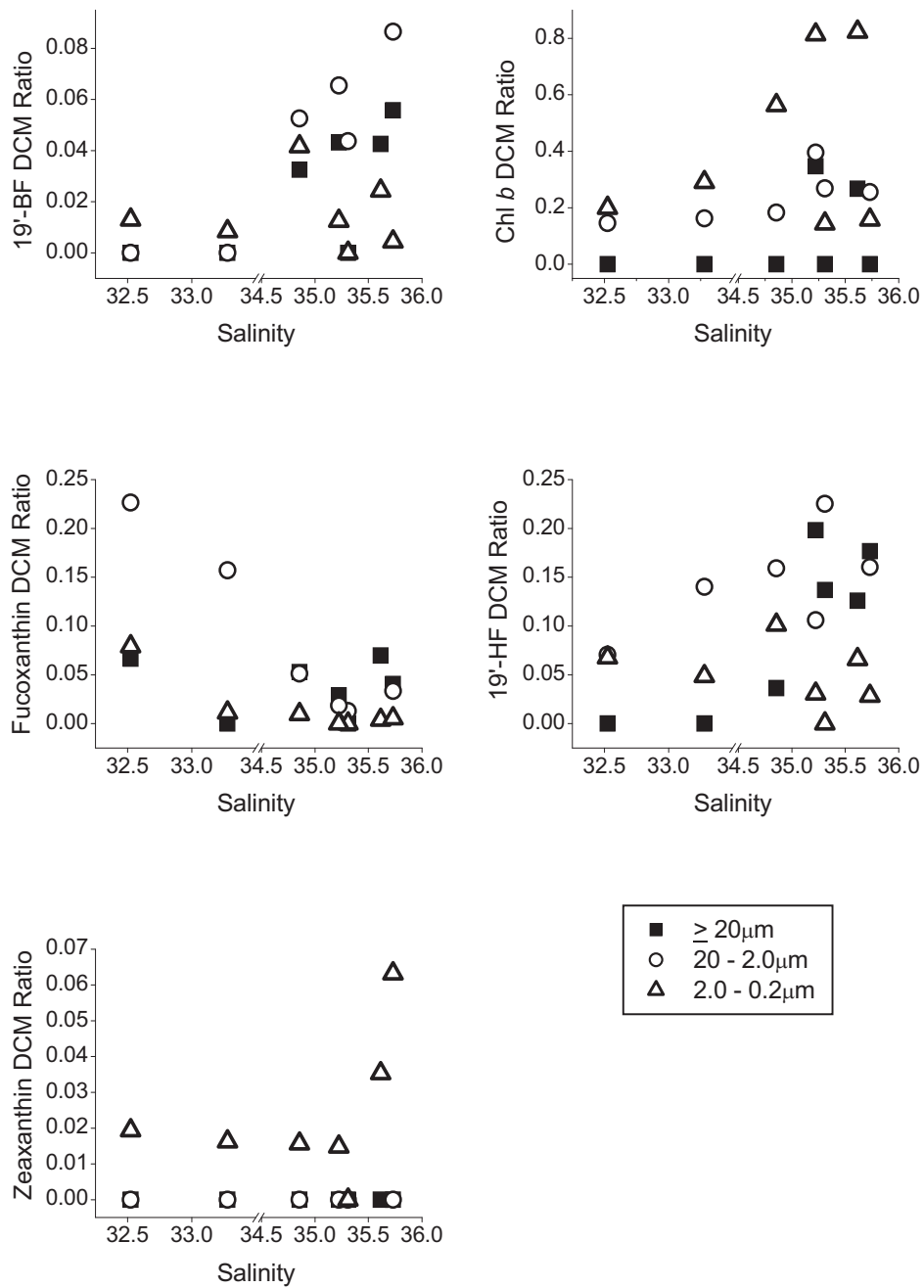


Figure 24. Ratios of DCM taxonomic marker pigments to Chl *a* within the size fraction.

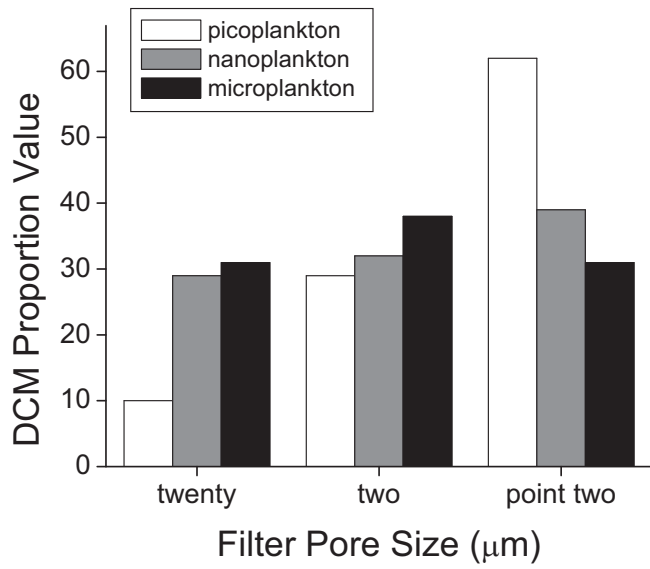
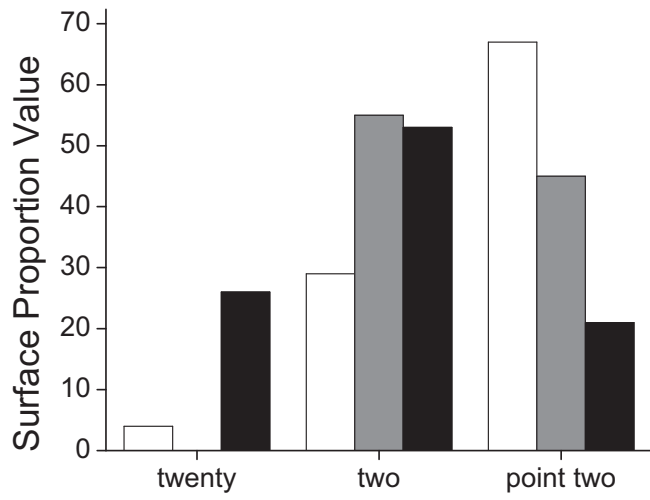


Figure 25. Proportion of taxonomic marker pigments within the operational size ranges contrasted to the pigment-based size classification.

Comparison of pigment-based estimation of phytoplankton size-class distribution to sequential filtration results.

Chl*a* biomass proportions of individual taxa found in size fractionated samples is expected to provide a more accurate description of the phytoplanktonic taxa present in the different size classes than the standard method of bulk GF/F filtration followed by HPLC analysis. In order to assess the accuracy of this assumption we compared the results obtained bulk by GF/F filtrations with those obtained from sequential filtration using the operational size class distribution which corresponds to pore sizes of 20µm, 2.0µm and 0.2µm (Sieburth et al., 1978). For this purpose Chl*a* concentrations obtained from GF/F filters correspondent to the biomass proportion of the operational size classes, the estimated Chl*a* biomass proportion ($eBP_{Chl a}$), was calculated using the formulation of Vidussi et al. (2001). In turn, the fractionated Chl*a* biomass proportion $fBP_{Chl a}$ for total Chl*a* concentration found in each size fraction of the samples filtered using tandem filtration was calculated.

$$i fBP_{Chl a} = \Sigma Chl a \text{ (mg/m}^3\text{)} \quad (5)$$

$$i eBP_{Chl a} = BP_{(i)} \times Chl a \text{ (mg/m}^3\text{)} \quad (6)$$

Where i = micro, nano and pico size classes.

Considering that Chl*a* biomass proportions found in the size fractionated samples ($fBP_{Chl a}$) corresponds to a more accurate description of the biomass attributed to the size classes, application of the standard method led to underestimation of microplankton biomass (micro $eBP_{Chl a}$) in the mid and far-fields (Fig. 26). On the other hand, near-field

samples showed a very significant overestimation of microplankton¹. Mid and far-field nano $eBP_{Chl a}$ showed an overestimation in biomass (Fig. 27) while pico $eBP_{Chl a}$ showed a slight overestimation in the far-field, however, there was a significant overestimation within the near-field (Fig. 28). This comparison shows that caution should be exercised in estimating taxonomic biomass contributions to operational size classes using bulk GF/F filtration. Tandem filtration using different pore sizes is advised.

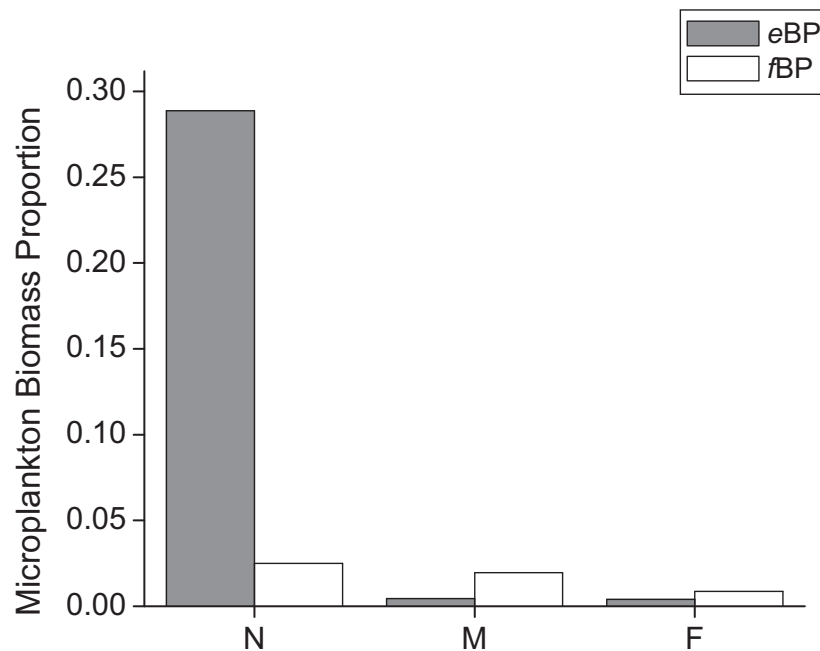


Figure 26. Estimated and fractionated microplankton $Chl a$ biomass proportions. Results show a significant overestimation for microplankton in the near-field, while mid and far-fields demonstrate an underestimation of microplanktonic biomass.

¹ Note: Peak resolution of fucoxanthin at station 9_1 was very poor. Non the less, fucoxanthin concentration was calculated with available data based on the premise that all other samples taken at that station showed no evidence of the presence of other pigments that might have co-eluted.

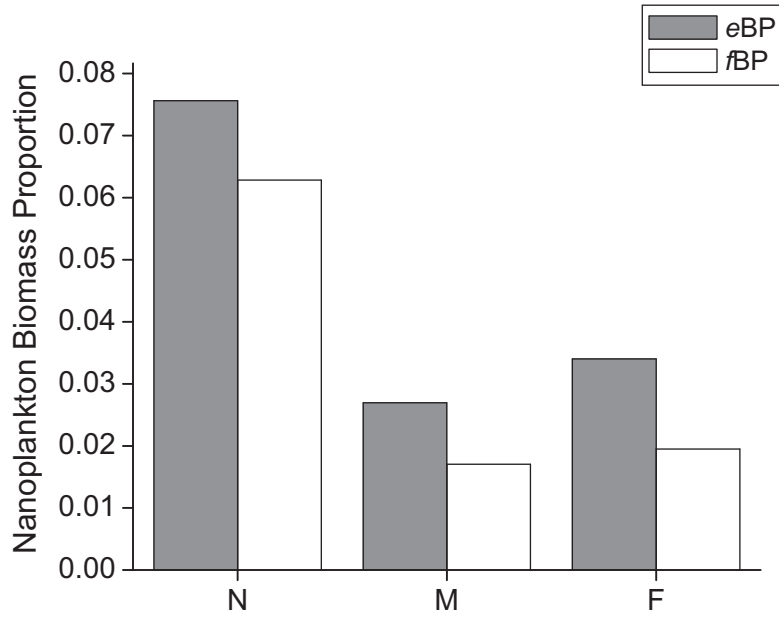


Figure 27. Estimated and fractionated nanoplankton Ch a biomass proportions. Results show overestimation for nanoplankton biomass in the near, mid and far-fields.

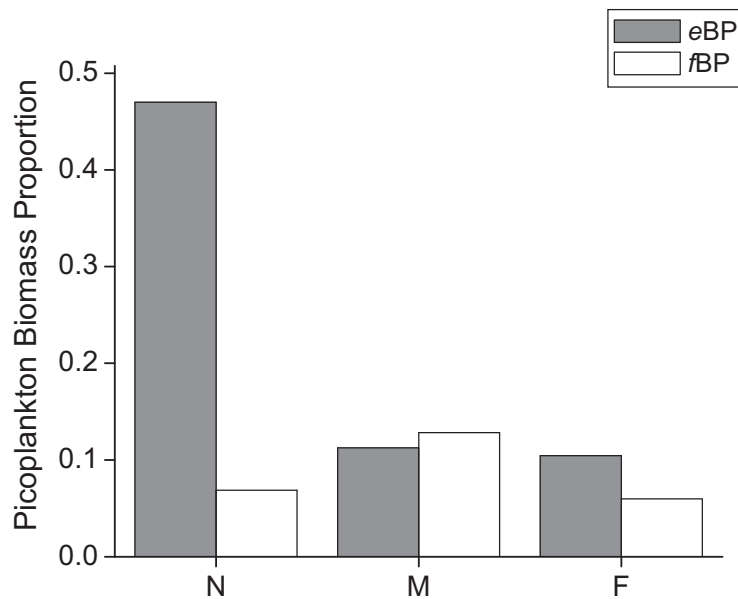


Figure 28. Estimated and fractionated picoplankton Ch a biomass proportions. Results show a significant overestimation for picoplankton in the near-field, with a slight over estimation in the far-field. Mid-field shows a slight underestimation of picoplanktonic biomass.

Determining proportional recovery of fractionated samples.

In order to provide a view of the effect of fractionation on sample recovery the sum concentration of Chl *a* from fractionated samples was compared to that obtained from GF/F samples and reported as the proportion recovered follows:

$$\text{Proportional Recovery} = \frac{\sum \text{fractionated Chl } a_{(i)}}{\text{Chl } a_{(GF/F)}} \times 100 \quad (7)$$

As the 0.2 μm filter is expected to retain the smallest picoplankton lost to the GF/F filter with an operational pore size of 0.7 μm , the sum of the fractionated samples should yield greater recovery. Results were variable, showing such increased recovery mostly for surface samples. DCM samples showed good recovery in the mid-field. However poor recovery (<50) was found in far-field samples for both surface and DCM (Fig. 29).

Reduction of filtration time could greatly increase the percent recovery for samples since pigments are photosensitive and exposure to artificial light and pigment degradation would be reduced. Hence, fractionated filtration does have its challenges. Yet, results also indicate that although chemotaxonomy is very useful in determining phytoplankton classes, it is unable to infer on phytoplankton size structure.

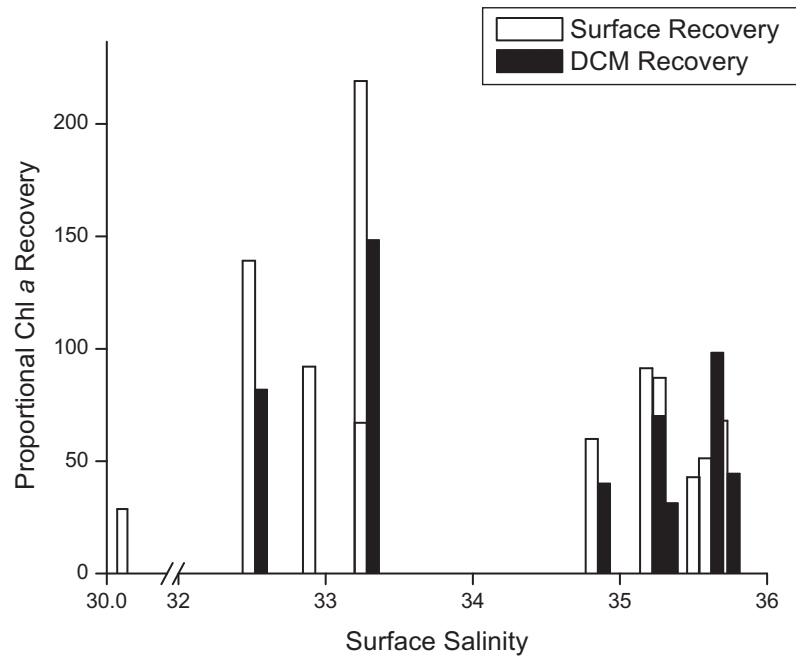


Figure 29. Proportional recovery values for Chl*a*.

Therefore, if identification of phytoplankton specie population is wanted, standard chemotaxonomy using GF/F filters is adequate (Vidussi et al., 2001; Jeffery et al., 1997). In situations where biomass contribution from each size class is needed, fractionated fluorometric analysis would suffice as long as it coupled with microscopic analysis and samples are carefully filtered. Prior filtration of samples using a 20-200 μ m mesh would be prudent. Nonetheless, if specific phytoplankton community composition and size class structure is in question then fractionated filtration coupled with HPLC analysis is recommended.

VII. Conclusions

This study showed little response to the effect of cyclonic and anticyclonic eddies in phytoplankton population and abundance. However, a slight increase in pico and nanoplankton biomass was noted, with values higher in the cyclonic region than the anticyclonic region.

Biomass proportions, as derived from GF/F filtrations, showed a dominance of picoplankton throughout the salinity gradient. A decline was observed for both nano and picoplankton as we approach the river plume, more so in the case of nanoplankton biomass proportion. Subsequently, microplankton biomass significantly increased.

Community size structure determined by sequential fractionation revealed the presence of taxonomic marker pigments throughout the size ranges. This suggests that community size structure cannot be accurately determined based exclusively on chemotaxonomy. Comparison of *Chl a* biomass proportion as derived from GF/F filtrations (*eBP*) with that derived from sequential filtrations (*fBP*) suggests that *eBP* can considerably over estimate or under estimate the influence of community size structure within phytoplankton populations.

Proportional recovery values from fractionated and bulk filtrations for *Chl a* were variable. However, if specific size structure of phytoplanktonic populations is in question, sequential filtration using designated pore sizes coupled with HPLC is suggested.

VIII. References

- Andersen, R.A., Bidigare, R.R., Keller, M.D., Latasa, M., 1996. A comparison of HPLC pigment signatures and electron microscopic observations for oligotrophic waters of the North Atlantic and Pacific Oceans. *Deep-Sea Res. (II)*, 43, No. 2-3, p.517-537
- Barlow, R.G., Mantoura, R.F.C., Cummings, D.G., Fileman, T.W., 1997. Pigment chemotaxonomic distributions of phytoplankton during summer in the western Mediterranean. *Deep-Sea Res. (II)*, 44, No. 3-4, p.833-850
- Barlow, R.G., Mantoura, R.F.C., Gough, M.A., Fileman, T.W., 1993. Pigment signatures of the phytoplankton composition in the northeastern Atlantic during the 1990 spring bloom. *Deep-Sea Res. (II)*, 40, No. 1/2, p. 459-477
- Bidigare, R.R., Nelson, C., Leonard, C.L., Quay, P.D., Parsons, M.L., Foley, D.G., Seki, M.P., 2003. Influence of a cyclonic eddy on microheterotroph biomass and carbon export in the lee of Hawaii. *Geophysical Res. Letters*, 30, No. 6, p.51_1 – 51_4
- Bidigare, R.R., Ondrusek, M.E., Brooks, J.M., 1993. Influence of the Orinoco River outflow on distributions of algal pigments in the Caribbean Sea. *J. of Geophys. Res.*, 98, C2, 2259-2269
- Bricaud, A., Claustre, H., Ras, J., Oubelkheir, K., 2004. Natural variability of phytoplankton absorption in oceanic waters: Influence of the size structure of algal populations. *J. of Geophys. Res.*, 109, C11010
- Brown, S.L., Landry, M.R., Selph, K.E., Yang, E.J., Rii, Y.M., Bidigare, R.R., 2008. Diatoms in the desert: Plankton community response to a mesoscale eddy in the subtropical North Pacific. *Deep-Sea Res. (II)*, 55, 1321-1333
- Cárdenas González, O.E., 2006. Determinación de la distribución espacio-temporal de poblaciones fitoplanctónicas del mar Caribe utilizando pigmentos fotosintéticos. Unpublished. Personal communication, Dr. Jorge Corredor, Dept. of Marine Sciences, University of Puerto Rico, Mayagüez, PR
- Corredor, J., Morell, J., López, J., Armstrong, R., Dieppa, A., Cabanillas, C., Cabrera, A., Hensley, V., 2003. Remote continental forcing of phytoplankton biogeochemistry: Observations across the "Caribbean-Atlantic front". *Geophys. Res. Lett.*, 30, No. 20, p. 2057
- Corredor, J.E., Morell, J., Mendez, A., 1984. Dissolved nitrogen, phytoplankton biomass and island mass effects in the northeastern Caribbean Sea. *Carib. J. Sci.*, 20, No. 3-4, p. 129-137

- Corredor, J.E., Morell, J.M., 2001. Seasonal variation of physical and biogeochemical features in eastern Caribbean Surface Water. *J. Geophys. Res.*, 106, C3, p. 4517 – 4525
- Corredor, J.E., Morell, J.M., Lopez, J.M., Capella, J.E., Armstrong, R.A., 2004. Cyclonic Eddy Entrainment of Orinoco River Plume in Eastern Caribbean. *EOS*, 85, p. 197-201
- Craig, S.R., 1986. Picoplankton size distributions in marine and fresh waters: problems with filter fractionation studies. *FEMS Microbiology Letters*, 38, No.3, p. 171-177
- Del Castillo, C.E., Coble, P.G., Morell, J.M., López, J.M., Corredor, J.E., 1999. Analysis of the optical properties of the Orinoco River plume by absorption and fluorescence spectroscopy. *Marine Chemistry*, 66, p. 35-51
- Ducklow, H.W., Steinberg, D.K., Buesseler, K.O., 2001. Upper ocean carbon export and the biological pump. *Oceanography*, 14, No.4, p. 50-58
- EDOCC, 2001. Ecological Determinants of Oceanic Carbon Cycling (EDOCC): A Framework for Research. <http://picasso.oce.orst.edu/ORSOO/EDOCC/>
- Foster, R. A., Subramaniam, C., Mahaffey, E. J., Carpenter, D. G., Capone, J. P., Zehr, 2007. Influence of the Amazon River plume on distributions of free-living and symbiotic cyanobacteria in the western tropical north Atlantic Ocean. *Limnol. Oceanogr.*, 52, No.2, p. 517-532
- Geider, R.J., 1988. Abundances of autotrophic and heterotrophic nanoplankton and the size distribution of microbial biomass in the southwestern North Sea in October 1986. *J. of Experimental Marine Biology and Ecology*, 123, No.2, p. 127-145
- Gieskes, W.W.C., Kraay, G.W., Nontji, A., Setiapermana, D., Sutomo., 1988. Monsoonal alternation of a mixed and a layered structure in the phytoplankton of the euphotic zone of the Banda Sea (Indonesia): a mathematical analysis of algal pigment fingerprints. *Neth. J. of Sea Res.*, 22, No.2, p. 123-137
- Guzmán, J., Claustre, H., Marty, J., 1995. Specific phytoplankton signatures and their relationship to hydrographic conditions in the coastal northwestern Mediterranean Sea. *Mar. Ecol. Prog. Ser.*, 124, p. 247-258
- Graham, L.E., Wilcox, L. W., 2000. *Algae*. Prentice Hall, 640p
- Hashihama, F., Hirawake, T., Kudoh, S., Kanda, J., Furuya, K., Yamaguchi, Y., Ishimaru, T., 2008. Size fraction and size composition of phytoplankton in the Antarctic marginal ice zone along the 140°E meridian during February - March 2003. *Polar Science*, 2, p. 109-120
- Jeffery, S.W., 1976. A report of green algal pigments in the central North Pacific Ocean. *Marine Biology*, 37, p. 33-37

- Jeffery, S.W., Mantoura, R.F.C., Wright, S.W., 1997. Phytoplankton pigments in oceanography: guidelines to modern methods. UNESCO Publishing, 661pp
- Karger-Muller, F.E., Castro, R. A., 1994. Mesoscale processes affecting phytoplankton abundance in the southern Caribbean Sea. *Continental Shelf Res.*, 14, No. 2/3, p. 199-221
- Lance, V.P., Hiscock, M.R., Hilting A.K., Stuebe, D.A., Bidigare, R.R., Smith, W.O.Jr., Barber R.T., 2007. Primary productivity, differential size fraction and pigment composition responses in two Southern Ocean in situ iron enrichments. *Deep-Sea Res. (I): Oceanographic Res. Papers*, 54, No.5, p. 747-773
- Li, H., Gong, G., Hsiung, T., 2002. Phytoplankton pigment analysis by HPLC and its application in algal community investigations. *Bot.Bull.Acad.Sin.*, 43, p. 283-290
- Lima, I.D., Olson, D.O., Doney, S.C., 2002. Biological response to frontal dynamics and mesoscale variability in oligotrophic environments: A numerical modeling study. *J Geophys. Res.*, 10.1029/2000JC000393, 1-21
- López Rosado, R., 2008. Photosynthetic efficiency of phototrophic plankton and bio-optical variability as influenced by mesoscale processes in the Eastern Caribbean Basin. Doctor of Philosophy, University of Puerto Rico, Mayaguez, PR
- Malone, T.C., 1971. The relative importance of nanoplankton and netplankton as primary producers in tropical oceanic and neritic phytoplankton communities. *Limnol. Oceanogr.*, 16, No.4, p. 633-639
- Marañón, E., Holligan, P.M., Barciela, R., González, N., Mouriño, B., Pazó, M.J., Varela, M., 2001. Patterns of phytoplankton size structure and productivity in contrasting open-ocean environments. *Mar. Ecol. Prog. Ser.*, 216, p.43-56
- Marra, J., Barber, R.T., 2004. Phytoplankton and heterotrophic respiration in the surface layer of the ocean. *Geophysical Res. Letters*, 31, L09314
- Marra, J., Trees, C.C., O'Reilly, J.E., 2007. Phytoplankton pigment absorption: A strong predictor of primary productivity in the surface ocean. *Deep-Sea Res. (I)*, 54, p. 155-163
- Martin, A.P., Pondaven, P., 2003. On estimates for the vertical nitrate flux due to eddy pumping. *J. of Geophys. Res.*, 108, C11, p. 23-1 - 23-10
- Martin, A.P., Richards, K.J., 2001. Mechanisms for vertical nutrient transport within a North Atlantic mesoscale eddy. *Deep-Sea Res. (II)*, 48, p. 757, 773
- Martin-Cereceda, M., Novarino, G., Young, J.R., 2003. Grazing by *Prymnesium parvum* on small planktonic diatoms. *Aquat. Microb. Ecol.*, 33, p.191-199

Mcguillicuddy, D.J.Jr., Anderson, L.A., Bates, N.R., Bibby, T., Buessler, K.O., Carlson, C.A., Davis, C.S., Ewart, C., Falkowski, P.G., Goldthwait, S.A., Hansell, D.A., Jenkins, W.J., Johnson, R., Kosnyrev, V.K., Ledwell, J.R., Li, Q.P., Siegal, D.A., Steinberg, D.K., 2007. Eddy/Wind Interactions Stimulate Extraordinary Mid-Ocean Pankton Blooms. *Science*, 316, p. 1021-1026

Mcguillicuddy, D.J.Jr., Robinson, A.R., Siegal, D.A., Jannasch, H.W., Johnson, R., Dickey, T.D., McNeil, J., Michaels, A.F., Knap, A.H., 1998. Influence of mesoscale eddies on new production in the Sargasso Sea. *Nature*, 394, 263-266

Moore, L.R., Goericke, R., Chisholm, S.W., 1995. Comparitive physiology of *Synechococcus* and *Prochlorococcus*: influence of light and temperature on growth, pigments, fluorescence and absorptive properties. *Mar. Ecol. Prog. Ser.*, 116, p. 259-275

Morell, J.M., Corredor, J.E., 2001, Photomineralization of fluorescent dissolved organic matter in the Orinoco River plume: Estimation of ammonium release. *J. of Geophys. Res.*, 106, C8, p. 16,807-16,813

Oschlies, A., Garcon, V., 1998. Eddy-induced enhancement of primary production in a model of the North Atlantic Ocean. *Nature*, 394, p. 266-269

Philander G. S., 1990. *El Niño, La Niña, and the Southern Oscillation*. Academic Press, p. 68-70

Pressinotto, R., Duncombe Rae, C.M., 1990. Occurrence of anticyclonic eddies on the Prince Edward Plateau (Southern Ocean): effect on phytoplankton biomass and production. *Deep-Sea Res.*, 37, No.5, p. 777-793

Ricahrdson, T. L., Jackson, G.A., 2007. Small phytoplankton and carbon export from the surface ocean. *Science*, 315, p. 838

Rivkin, R.B., Legendre, L., 2002. Roles of food web and heterotrophic microbial processes in upper ocean biogeochemistry: Global patterns and processes. *Ecol. Res.*, 17, p. 152-159

Rodriguez, F., Varela, M., Fernández, E., Zapata, M., 2003. Phytoplankton and pigment distribution in an anticyclonic slope water oceanic eddy (SWODDY) in the southern Bay of Biscay. *Marine Biology*, 143, p. 995-1011

Roy, R., Pratihary, A., Mangesh, G., Naqvi, S.W.A., 2006. Spatial variation of phytoplankton pigments along the southwest coast of India. *Estuarine, Coastal and Shelf Sci.*, 69, p. 189-195

Sander, E., 1981. A preliminary assesment of the main causative mechanisms of the "Island Mass" effect of Barbados. *Mar. Biol.*, 64, p. 199-205

- Sieburth, J., Smetacek, V., Lenz, J., 1978. Pelagic ecosystem structure: Heterotrophic compartments of the plankton and their relationship to plankton size fractions. *Limnol. Oceanogr.*, 23, No.6, p. 1256-1263
- Silva, A., Mendes, C.R., Palma, S., Brotas, V., 2008. Short-time scale variation of phytoplankton succession in Lisbon bay (Portugal) as revealed by microscopy cell counts and HPLC pigment analysis. *Estuarine, Coastal and Shelf Sci.*, 79, p. 230-238
- Smith, C.L., Richards, K.J., Fasham, M.J.R., 1996. The impact of mesoscale eddies on plankton dynamics in the upper ocean. *Deep-Sea Res. (I)*, 43, 11-12, p. 1807-1832
- Stockner, J.G., 1988. Phototrophic picoplankton: An overview from marine and freshwater ecosystems. *Limnol. Oceanogr.*, 33, No.4, 765-775
- Uitz, J., Claustre, H., Morel, A., Hooker, S.B., 2006. Vertical distribution of phytoplankton communities in open ocean: An assesment based on surface chlorophyll. *J. of Geophys. Res.*, 111, C08005
- Vaillancourt, R.D., Marra, J., Seki, M.P., Parsons, M.L., Bidigare, R.R., 2003. Impact of a cyclonic eddy on phytoplankton community structure and photosynthetic competency in the subtropical North Pacific Ocean. *Deep-Sea Res. (I)*, 50, p. 829-847
- Vidussi, F., Claustre, H., Manca, B.B., Luchetta, A., Marty, J., 2001. Phytoplankton pigment distribution in relation to upper thermocline circulation in the eastern Mediterranean Sea during the winter. *J. of Geophys. Res.*, 106, C9, p. 19,939-19,956
- Wawrik, B., Paul, J.H., 2004. Phytoplankton community structure and productivity along the axis of the Mississippi River plume in oligotrophic Gulf of Mexico waters. *Aquat Microb Ecol*, 35, p. 185-196
- Whitney, F., Robert, M., 2002. Structure of Haida eddies and their transport of nutrient from coastal margins into the NE Pacific Ocean. *J. of Oceanography*, 58, p. 715-723
- Williams, R.G., Follows, M.J., 1998. Eddies make ocean deserts bloom. *Nature*, 394, 228-229